NASA TN D-1310

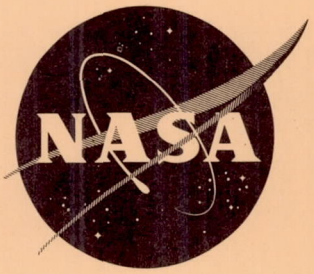

TECHNICAL NOTE

D-1310

OBSERVATIONS OF PROPERTIES OF SINTERED WROUGHT TUNGSTEN SHEET AT VERY HIGH TEMPERATURES

By E. C. Sutherland and William D. Klopp

Lewis Research Center
Cleveland, Ohio

NATIONAL AERONAUTICS AND SPACE ADMINISTRATION
WASHINGTON
February 1963

NATIONAL AERONAUTICS AND SPACE ADMINISTRATION

TECHNICAL NOTE D-1310

OBSERVATIONS OF PROPERTIES OF SINTERED WROUGHT TUNGSTEN SHEET AT VERY HIGH TEMPERATURES

By E. C. Sutherland and William D. Klopp

SUMMARY

The mechanical properties of tungsten sheet from five typical commercial lots were examined at temperatures from 3650° to 5200° F. The properties varied widely with the material lot as well as with the type of test. (The variations at very high temperatures appeared greater than those observed at lower temperatures.)

The presence of trace elements appears to affect significantly the properties of tungsten sheet. These impurities exert solid-solution-strengthening effects and grain-growth-inhibition effects, both of which influence the tensile and creep properties at elevated temperatures.

INTRODUCTION

With the present emphasis on higher operating temperatures in the missile and space-vehicle programs, it has become necessary to look critically at the contribution that refractory metals can make to the need for material strength at very high temperatures. Within the present state of the art, work with molybdenum, tantalum, and columbium has produced metals and alloys that have very promising properties up to 3000° F. At temperatures above 3500° F, most of these alloys do not have sufficient strength for structural applications. Tungsten appears to have the most potential for development as a high-strength material above 3500° F and may find application to at least 5000° F, since its melting point is 6170° F.

One factor limiting the application of tungsten metal at elevated temperatures is the lack of design data concerning its behavior at these temperatures. Previous work (ref. 1) presented the tensile properties of tungsten rod up to 4500° F, but there appears to be a near void on sheet data at temperatures near 5000° F.

Most of the structural applications of tungsten, within NASA interest, involve the use of this material in sheet form. Since properties of refractory sheet metal have frequently been observed to differ from those of rod and bar stock, an evaluation of the high-temperature mechanical properties of powder-metallurgy tungsten sheet was undertaken. Material from several different lots was studied, since work at the Lewis Research Center and elsewhere indicated sintered wrought tungsten had considerable property variation among lots.

In this investigation, five lots of tungsten from different suppliers were evaluated by tensile tests at temperatures ranging from 3650° to 5200° F. In addition, short-time stress-rupture properties at 4800° F were determined and the ductile-to-brittle transition temperature in a bend test was evaluated for each lot of material. The differences in mechanical properties are correlated with observed differences in microstructure and chemical composition.

MATERIALS

The materials as chosen were to be representative of typically pure tungsten sheet with normal processing variables. Five lots of commercially pure undoped tungsten sheet (99.9 percent tungsten, min.) processed by the powder-metallurgy method were therefore obtained from different sources. Processing history of the sheet was unavailable since most producers consider such information to be proprietary.

The material studied was 0.040 inch thick trimmed to 6 by 24 inches, except for lot E, which was 0.060 inch thick. Inspection of the as-received sheet showed that one sheet (lot A) had laminated edges. This edge material was discarded to a depth of 1/2 inch. The microstructure of the sheet from four lots showed the highly stressed fibrous structure typical of cold-worked tungsten metal (fig. 1), while the microstructure of the remaining sheet (lot D, fig. 1(d)) indicated that the sheet had been given a partial recrystallization anneal.

All the materials were given complete spectrographic analyses, and chemical determinations were made for carbon, sulfur, oxygen, hydrogen, and nitrogen. The analyses are given in table I. Average pycnometric densities determined for three stress-rupture samples from each lot after testing are included.

APPARATUS AND PROCEDURE

Test Specimens

Sheet specimens of the type shown in figure 2 were used in this study. In order to minimize fabrication costs, rectangular specimens

with no reduced test section were used for the high-temperature tensile tests. The specimens were prepared by cutting the as-received tungsten sheets with a 0.015-inch abrasive wheel with the test direction parallel to the final rolling direction of the sheet. The specimens were nominally 0.040 inch thick (0.060 in. for lot E), 0.625 inch wide, and 6 inches long (fig. 2(a)).

For the stress-rupture study, a standard sheet tensile specimen (fig. 2(b)), recommended in reference 2, was adopted, and a technique was employed whereby the specimen could be cut by a commercial electric-discharge machine. With proper design of the electrode and close control of operating conditions, the entire specimen was cut within the specified tolerance in one operation. Figure 3 shows the machine and tooling setup.

The bend-test specimens were cut in the same manner as the tensile-test specimens but were 0.040 inch thick (0.060 in. for Lot E), 0.625 inch wide, and 1.5 inches long (fig. 2(c)).

High-Temperature Stress-Rupture Tests

Stress-rupture studies were conducted in vacuum ($< 1 \times 10^{-4}$ mm Hg) at 4800° F on a conventional constant-load beam machine (fig. 4). In order to accommodate sheet specimens, the equipment was modified from the usual cylindrical heating element to a flattened tube-type heater. The overall dimensions of this heater (fig. 5) were approximately 0.375 by 1 by 3 inches. The center of the 0.375-inch dimension contained a slot 0.0625 inch wide and 2.375 inches long. Use of the relatively short heater permitted the 6-inch-long strip specimen to be gripped outside the heating element by 0.25-inch-diameter pins in 1-inch-diameter tungsten grips. Extension of the specimens was measured from loading rod movement.

At high temperatures, vaporization of tungsten caused relatively rapid deterioration of the tungsten heating elements and limited the stress-rupture tests at 4800° F to a maximum of 500 minutes. (Evaporation of tungsten leads to development of a hot spot and subsequent localized melting of the heating element.)

The average grain diameter of the tungsten sheet specimens after stress-rupture testing was determined by metallographically counting, in at least three areas, the number of grain boundary intercepts n with a circle 48.3 centimeters in circumference C at a magnification M of 250. The average grain diameter L was calculated from the relation

$$L = \frac{C}{(n - 1)M}$$

High-Temperature Tensile Tests

Tensile tests were conducted in vacuum ($\sim 1 \times 10^{-4}$ mm Hg) at temperatures ranging from 3650° to 5200° F with test equipment (fig. 6) and techniques described previously (ref. 3). The methods of specimen gripping and heating were the same as those used for the stress-rupture tests.

The effective gage length was determined by the temperature profile of the specimen. Temperature measurements indicated that the zone of constant temperature at the center of the specimen was approximately 1.125 inches long, and an effective gage length of 0.5 inch was used. This area was marked by resistance welding two 0.010-inch-diameter tungsten wires across the edge of the specimen (fig. 2(a)).

The tensile specimens were brought to temperature in 15 to 25 minutes, soaked for 2 minutes, and then pulled to fracture at a constant crosshead speed of 0.030 inch per minute, which gave a strain rate during plastic flow of approximately 0.020 inch per inch per minute in the gage length.

The average grain diameters of the tensile specimens were determined after testing by the grain-boundary intercept method described previously.

Bend Tests

Bend tests were conducted on a commercial hydraulic-driven compression machine (fig. 7) with a test fixture designed in accordance with recommendations of reference 4. The bend radius was selected as four times the sheet thickness, or 0.160 inch. Heating (in air atmosphere) was achieved by surrounding the fixture and the specimen with a small resistance-wound muffle furnace. Temperatures were determined with a thermocouple located directly below and within 1/32 inch of the specimen. The apparatus was brought to a constant temperature and soaked for 10 minutes before testing. The specimen was bent at a crosshead speed of 4 inches per minute until fracture occurred, or to a bend angle of at least 120°. Ductility was measured as a percentage of the 120° angle before fracture.

RESULTS AND DISCUSSION

Stress-Rupture Properties

Data from stress-rupture studies at 4800° F on the five lots of commercial tungsten sheet are presented in table II. The variations in second-stage (minimum) creep rate $\dot{\epsilon}$ and rupture life t_r with stress

σ are shown in figure 8. Data at 4892° F on commercial powder-metallurgy tungsten from an earlier study (ref. 5) are included for comparison.

It is apparent that the stress-rupture properties vary considerably among lots. The stresses for equivalent creep rates and rupture lives for lots A and B are approximately double those for lots C and E. For comparison, data from reference 5 on powder metallurgy tungsten indicate creep strengths intermediate to those of lots B and D in the present study. Although the data from reference 5 are at a slightly higher temperature, 4982° F, they may be interpolated to 4800° F by using the observed creep activation energy of 160,000 calories per mole. This correction does not change significantly the position of these data relative to lots B and D.

The dependency of creep rate and rupture life on stress is seen to differ between the present study and the earlier study (ref. 5). In the present study, a fifth-power dependency on stress, as suggested by the recent review by Sherby (ref. 6), adequately correlated both the creep rates and rupture lives for each lot. In contrast, in reference 5 it was observed that the creep rates varied according to the 6.5 power of stress. Sherby also concluded that, at high temperatures, the creep rate varies with the square of the grain size. This conclusion is in distinct contrast to earlier observations (refs. 7 and 8), which indicate that large-grained materials exhibit lower creep rates at high temperatures than do fine-grained materials. The relation derived by Sherby is

$$\dot{\epsilon} = SL^2D\left(\frac{\sigma}{E}\right)^5 \qquad (1)$$

where

$\dot{\epsilon}$ creep rate, sec^{-1}
S constant = 10^{29} cm^{-4}
L average grain diameter, cm
D self-diffusion rate, $(cm^2)(sec^{-1})$
σ stress, psi
E modulus of elasticity, psi

Although comparison of the observed creep rates with the calculated creep rates is not possible because of lack of data on the high-temperature modulus of polycrystalline tungsten, equation (1) predicts that creep rate varies directly as the self-diffusion rate and as the square of the grain diameter. In order to determine the relation between creep rates and grain sizes, the average stress creep-rate parameter $\dot{\epsilon}\sigma^{-5}$ is plotted against the average grain diameter for each of the five tungsten lots in figure 9. It is seen that a line of slope 0.5, as predicted

by equation (1), approximately correlates the data for lots A, B, C, and D but not for lot E. The stress creep-rate parameter for lot E is quite high in relation to the parameters for lots A, B, and D, which exhibited about the same grain size.

A plot of creep rate compensated for average lot grain size $\dot{\epsilon}L^{-2}$ against stress σ is shown in figure 10. In contrast to the relatively large creep-rate differences shown in figure 8, the modified data for lots A, B, C, and D fall in a narrow band through which a single line of slope 0.2, as predicted by equation (1), may be fairly drawn. These data indicate that the stress-rupture property variation among these lots is primarily a result of their different grain sizes. The data for lot E generally fall below this line, which indicates that the properties of this lot are affected by a factor in addition to grain size.

It is apparent from the preceding discussions that the creep-rupture properties of lots A, B, C, and D, while showing considerable variation among lots, are adequately correlated by the introduction of the grain size factor described by Sherby. The properties of lot E, which showed relatively low creep strength, are not correlated by this factor. However, consideration of the residual impurity levels for the various lots, as given in table I, shows that lot E was relatively impure, especially with regard to oxygen, carbon, aluminum, chromium, nickel, and silicon contents. Since creep is assumed to be controlled by the rate of self-diffusion, the presence of these impurities apparently sufficiently distorts the atomic structure to affect significantly the self-diffusion rates and thus the creep rates.

It is of interest to note (table II) that, in lots A, B, D, and E, no grain growth could be detected during creep exposure. The data suggest that slight grain growth may have occurred during testing of lot C, although the observed grain size increases are judged within the error limits for grain size measurement. This behavior is attributed to minute compositional differences among the various lots. It is well known that undetectable impurities, often sodium salts added as "doping" agents, affect significantly the grain growth characteristics of tungsten. Although the five lots of tungsten in this study were nominally "undoped," it is considered probable that the minor amounts of residual impurities in each lot produce fine precipitate particles that tend to restrict grain growth. Electron photomicrographs of material from lots B, C, and E (fig. 11) tend to confirm the relation of grain growth to the presence of impurity particles. Lot C, which had the largest grain size, is seen to be relatively "clean," while lot E, with a much finer grain size, contained visible particles at the grain boundaries.

High-Temperature Tensile Tests

The results of the short-time tensile tests are given in table III and are shown in figure 12. The average grain diameters, measured after testing just inside the specimen hot zone, are included in table III and are also presented in figure 13. Representative microstructures from the fracture areas of the various specimens are shown in figure 14.

The high-temperature tensile properties of tungsten are seen to vary considerably from one lot to another in a manner similar to that observed for the creep-rupture properties. A significant difference exists, however, in that lot E, which exhibited low creep strength, displayed the highest tensile strength. Both the yield and ultimate tensile strengths of lot E were approximately three times higher than those of lot C (see fig. 12(b)). All lots, however, exhibited the normal decrease in strength with increasing temperature, with exception of a small increase in the strength of lot A in the vicinity of 4670° F.

Marked differences in the tensile ductilities of the five lots were observed, as indicated in figure 12(c). Lot C, which had the lowest tensile strength, exhibited very high ductilities and knife-edge fractures at all temperatures from 3640° to 5270° F. This material also exhibited abnormal grain growth resulting in exceedingly large grains in the fracture area (figs. 14(a) and (c)). This grain growth is apparently associated with the large amount of plastic deformation accompanying necking and fracture. Lots A, B, and D, which had similar strengths below 4600° F, showed moderately increasing ductilities above 3800° F. This behavior is typical of powder-metallurgy tungsten, which normally exhibits a ductility minimum in the range from 3600° to 4000° F (refs. 1 and 9). Ductility in this range increases with increasing strain rate (ref. 9), which suggests that the minimum may be associated with diffusion of an unidentified impurity, analogous to the frequently observed low-temperature strain-aging phenomenon associated with interstitial impurities.

At 4900° and 4980° F, lot A showed a sharp increase in ductility as compared with the lower temperatures. The fractures at the high temperatures had a knife-edge appearance, similar to those observed for lot C. Abnormal grain growth also occurred near the fracture under these conditions, as shown in figure 14(d). Concurrent with the sharp increase in ductility and the abnormal grain growth in the fracture area, lot A showed an increase and then a decrease in strength with increasing temperature relative to lots B and D.

Lot E, in addition to being the strongest of the five lots studied, displayed contrasting ductility behavior. Although the other four lots showed high or increasing ductility over the temperature range studied, the ductility of lot E decreased significantly from 4040° to 4940° F

(fig. 12(c)). This behavior appears to be associated with the relatively high impurity content of lot E. As seen in table I, this lot had the highest analyzed levels of oxygen, carbon, aluminum, chromium, nickel, and silicon. If it is assumed that the normal ductility minimum at 3500° to 4000° F in powder-metallurgy tungsten is related to the diffusion rate of an impurity such as iron, the low ductility of lot E at 5000° F may be similarly related to the diffusion rate of a different impurity, such as aluminum or silicon.

The strengths of lots A, B, C, and D appear related to the respective grain sizes, as measured away from the area of severe deformation. Although a quantitative correlation has not been attempted, it is seen that the yield and ultimate strengths decrease with increasing grain size. Lot C, the weakest lot, exhibited the largest grain size at all temperatures, while lot A, the strongest at temperatures below 4800° F (with exception of lot E), had a much finer grain size. It thus appears that grain size, which was shown to affect significantly the creep properties, also affects the tensile properties to a considerable degree.

The tensile strength of material from lot E appears to be strongly affected by its relatively high level of impurities, as discussed earlier with regard to creep properties and tensile ductility. The apparently anomolous combination of low creep strength and high tensile strength, which characterize lot E, is analogous to the behavior of iron-carbon alloys. Although carbon additions increase the tensile strength of iron, it was pointed out in reference 6 that carbon increases the self-diffusion rate and thus the creep rate of iron at a given stress. It is likely that one or more of the impurities in lot E, such as aluminum or silicon, similarly produce solution strengthening during tensile testing but increase the self-diffusion rate of tungsten and thus lower the creep strength.

Bend Test

Inasmuch as the transition temperature for ductile-to-brittle fracture is commonly used as an indication of sheet quality and formability, a test in bending was made on the five lots of material in the as-received condition. In this study it was of interest to determine what correlation, if any, there was among the low-temperature ductility, the high-temperature mechanical properties, and the chemical composition of the various lots. Results of the bend transition temperature studies are shown in figure 15. These tests showed that the ductile-to-brittle transition occurred over a very narrow temperature band for each specific lot. Lot A had the lowest transition temperature at 335° F. The remaining temperatures in increasing order were: lot C, 405° F; lot D, 455° F; lot E, 475° F; and lot B, 720° F. The high transition temperature for lot B was unexpected as it was not indicated by any previous

test. Also of interest was the effect of small laminations on the transition temperature. As noted earlier, the edges of lot A sheet had laminations probably caused by shearing. When this edge material was tested, the transition temperature was in excess of 800° F, compared with only 335° F for sound material from the same sheet. The 0.060-inch sheet of lot E was tested over the same 0.160-inch radius, which may possibly have caused the transition temperature to be a little high, but it was not expected to change appreciably with a radius four times the sheet thickness.

There does not appear to be any consistent correlation between bend transition temperature and high-temperature strength or ductility. Lot A, which had the lowest transition temperature, had average high-temperature strength, while lot B, which had a transition temperature nearly 400° F higher, had essentially the same strength as lot A in the high-temperature tests. At the same time, lot C had a higher transition temperature than lot A but very low high-temperature strength. The lowest transition temperatures, however, are associated with lots A and C, which also exhibited explosive grain growth and excellent ductility at about 4900° F.

The analytical data of table I suggest a correlation between transition temperatures and chemical composition. If lot E is eliminated, the transition temperature of the various lots increases with increasing oxygen content. A similar relation may be noted with the hydrogen content (fig. 16). It is generally assumed that the presence of this element, in the very small quantities in which it occurs in tungsten, is not detrimental; however, the sixfold increase in hydrogen between lots A and B may have contributed to the large difference in transition temperature.

Little correlation is apparent between microstructure and transition temperature for the lots of tungsten evaluated in this study. Ordinarily, a heavily fibered microstructure is associated with low-temperature ductility; however, lot D, which appears to be partly recrystallized (fig. 1), had a ductile-to-brittle transition temperature lower than that of lots B and E, which exhibited heavily fibered structures.

CONCLUSIONS

The following conclusions are drawn from a study of the high-temperature mechanical properties of tungsten sheet from five different commercial sources:

1. The stress-rupture properties at 4800° F and tensile properties of commercial tungsten sheet at 3640° to 5270° F vary significantly from

one lot to another. Twofold variations in rupture strengths and tensile strengths were observed. The ductile-to-brittle bend transition temperatures of the as-received materials varied from 335° to 720° F.

2. The variations in creep and tensile strengths of lots A, B, C, and D are correlated with the grain sizes of the various lots as measured after testing. The grain size, in turn, appears to be controlled by the presence of impurity precipitates, which tend to restrict grain growth.

3. The variations in creep and tensile strengths of lot E relative to the four other lots studied are attributed to fairly high impurity levels in lot E. The high tensile strength of lot E may result from impurity solution strengthening. Conversely, these impurities apparently increase the self-diffusion rate of tungsten and greatly reduce the stress-rupture strength for lot E.

4. The ductile-to-brittle bend transition temperature increased with increasing oxygen and/or hydrogen content of the tungsten sheet.

Lewis Research Center
National Aeronautics and Space Administration
Cleveland, Ohio, September 13, 1962

REFERENCES

1. Sikora, Paul F., and Hall, Robert W.: High-Temperature Tensile Properties of Wrought Sintered Tungsten. NASA TN D-79, 1959.

2. Staff of National Academy of Sciences: Evaluation Test Methods for Refractory Metal Sheet Materials as Recommended by the Materials Advisory Board Refractory Metal Sheet Rolling Panel. Rep. MAB-176-M, Nat. Academy Sci., Sept. 6, 1961.

3. Hall, Robert W., and Sikora, Paul F.: Tensile Properties of Molybdenum and Tungsten from 2500° to 3700° F. NASA MEMO 3-9-59E, 1959.

4. Staff of National Academy of Sciences: Formability Screening Procedures as Recommended by the Formability Working Group of the MAB Subpanel on Evaluation of the Department of Defense Titanium Alloy Sheet Rolling Program. Rep. MAB-145-M, Nat. Academy Sci., May 29, 1959.

5. Green, Walter V.: Short-Time Creep-Rupture Behavior of Tungsten at 2250° to 2800° C. Trans. AIME, vol. 215, no. 6, Dec. 1959, pp. 1057-1060.

6. Sherby, Oleg D.: Factors Affecting the High Temperature Strength of Polycrystalline Solids. Acta Met., vol. 10, no. 2, Feb. 1962, pp. 135-147.

7. Sully, A. H.: Metallic Creep and Creep Resistant Alloys. Intersci. Publ., Inc., 1949.

8. Clark, Claude L.: High-Temperature Alloys. Pitman Publ. Corp., 1953.

9. Sikora, Paul F., and Hall, Robert W.: Effect of Strain Rate on Mechanical Properties of Wrought Sintered Tungsten at Temperatures Above 2500° F. NASA TN D-1094, 1961.

TABLE I. - ANALYSES AND DENSITIES OF COMMERCIAL TUNGSTEN FROM FIVE DIFFERENT SOURCES

[<, not detected and therefore less than quantity indicated.]

Element	Impurities, ppm				
	Lot				
	A	B	C	D	E
	Density, g/cc				
	19.22	19.23	19.24	19.22	19.25
Oxygen	5	19	8	13	29
Hydrogen	0.18	1.03	0.53	0.65	0.13
Nitrogen	28	17	18	24	6
Carbon	15	20	25	10	30
Sulfur	<10	<10	<10	10	<10
Aluminum	<2	<2	<2	<2	40
Boron	<2	<2	<2	<2	<2
Calcium	<10	<10	<10	<10	<10
Chromium	<5	<5	<5	<5	15
Copper	<1	<1	<1	<1	<1
Iron	30	20	10	15	10
Manganese	<1	<1	<1	<1	<1
Molybdenum	15	10	50	10	<10
Sodium	10	10	10	10	<10
Nickel	7	2	7	15	15
Lead	<10	<10	<10	<10	<10
Silicon	<3	<3	<3	<3	10
Tin	<5	<5	<5	<5	<3
Thorium	<30	<30	<30	<30	<30
Phosphorus	<20	<20	<20	<20	<20
Potassium	<10	<10	<10	<10	<10

TABLE II. - STRESS-RUPTURE PROPERTIES OF TUNGSTEN AT 4800° F

Lot	Stress, psi	Minimum creep rate, sec^{-1}	Rupture life, min	Average grain diameter, cm
A	1500	5.55×10^{-6}	319.3	2.9×10^{-3}
	1800	5.75×10^{-6}	240.4	2.8×10^{-3}
	2500	4.09×10^{-5}	39.2	3.2×10^{-3}
			Av. value	3.0×10^{-3}
B	1740	8.34×10^{-6}	155.7	3.7×10^{-3}
	1940	3.17×10^{-5}	70.1	4.5×10^{-3}
	2470	7.59×10^{-5}	22.9	4.5×10^{-3}
			Av. value	4.3×10^{-3}
C	720	3.33×10^{-6}	512	1.5×10^{-2}
	960	1.32×10^{-5}	208.8	1.4×10^{-2}
	1460	1.72×10^{-4}	13.2	1.2×10^{-2}
			Av. value	1.4×10^{-2}
D	1020	5.33×10^{-6}	>300	--------
	1550	1.17×10^{-5}	121.0	4.3×10^{-3}
	1800	2.97×10^{-5}	53.9	4.5×10^{-3}
	2500	3.08×10^{-4}	4.6	3.6×10^{-3}
	3000	1.02×10^{-3}	2.8	4.7×10^{-3}
			Av. value	4.3×10^{-3}
E	250	4.16×10^{-7}	>1000	--------
	670	1.42×10^{-6}	>460	--------
	1000	1.02×10^{-5}	91.8	3.3×10^{-3}
	1810	---------	5.9	--------
	1815	2.93×10^{-5}	7.5	3.5×10^{-3}
			Av. value	3.4×10^{-3}

TABLE III. - PROPERTIES OF TUNGSTEN FOR SHORT-TIME TENSILE TESTS

Lot	Test temperature, °F	Tensile strength, psi	Yield strength, psi	Reduction in area, percent	Elongation, percent	Average grain diameter, cm
A	3880	6950	4570	14.3	28.2	2.7×10^{-3}
	4040	5400	3500	21.6	25.0	---
	4150	5430	3530	29.4	27.3	2.5×10^{-3}
	4380	4500	2880	36.0	38.2	---
	4540	3480	2860	----	----	---
	4550	3730	----	36.2	37.5	---
	4670	3950	3300	47.8	42.5	2.9×10^{-3}
	4700	3600	----	46.2	48.5	---
	4900	2240	1910	99	31.3	3.8×10^{-3}
	4980	2060	1980	99	----	---
B	3870	6710	4070	12.2	20.6	---
	4040	5280	3270	31.0	42.5	3.2×10^{-3}
	4180	5350	3500	25.3	31.3	---
	4300	4650	3120	28.9	29.5	---
	4410	3650	2890	30.7	25.8	3.1×10^{-3}
	4680	3080	2230	33.3	40.6	4.4×10^{-3}
	4900	2750	2260	32.7	38.2	4.2×10^{-3}
C	3640	7070	3190	99	62.5	3.5×10^{-3}
	3870	6590	3330	99	62.5	3.4×10^{-3}
	4030	3770	2260	99	54.8	---
	4250	3120	1670	99	36.4	7.1×10^{-3}
	4410	2520	1250	99	65.1	7.7×10^{-3}
	4670	2150	960	99	49.2	9.5×10^{-3}
	4950	1750	900	99	54.8	1.40×10^{-2}
	5270	1335	675	--	----	---
D	3880	6200	3390	20.5	25.0	3.0×10^{-3}
	4020	5500	3160	28.5	28.4	---
	4230	3940	2840	31.3	34.3	3.7×10^{-3}
	4470	3520	2300	37.1	40.0	---
	4700	3000	2580	39.1	48.5	4.1×10^{-3}
	4960	2430	1960	41.6	----	4.2×10^{-3}
	5050	2440	1910	42.6	49.3	---
E	4040	6700	4530	47	48.5	2.3×10^{-3}
	4240	5510	4050	30.8	37.5	2.9×10^{-3}
	4440	5080	3860	31.7	35	---
	4700	4340	3490	17.4	22	2.6×10^{-3}
	4940	3620	3220	10.8	11	2.9×10^{-3}

(a) Lot A.

(b) Lot B.

(c) Lot C.

(d) Lot D.

(e) Lot E. C-60859

Figure 1. - Microstructures of five typical lots of tungsten in as-received condition. Etchant; KOH + $K_3Fe(CN)_6$; X250.

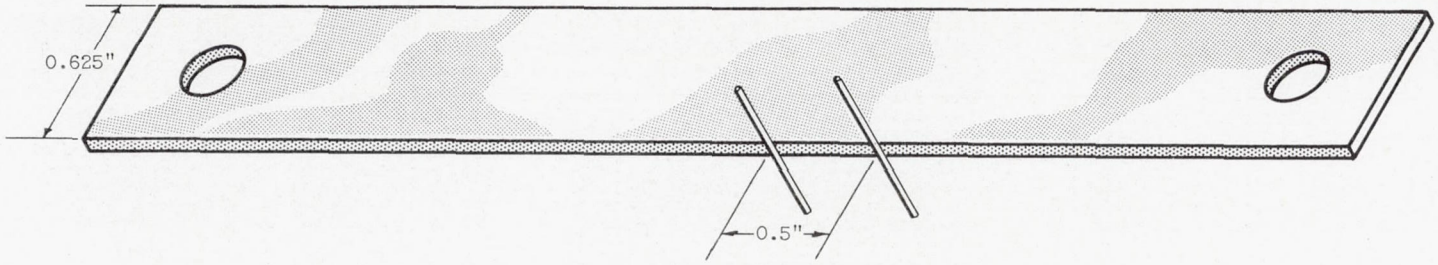

(a) Tensile specimen.

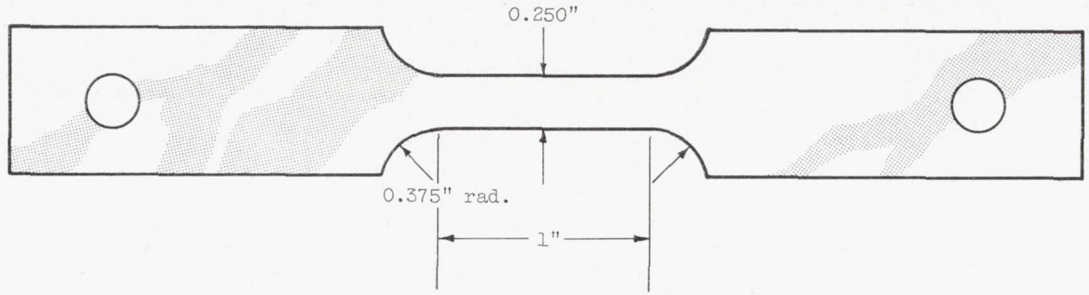

(b) Stress-rupture specimen.

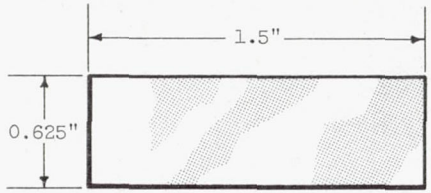

(c) Bend-test specimen.

CD-7357

Figure 2. - Test specimens.

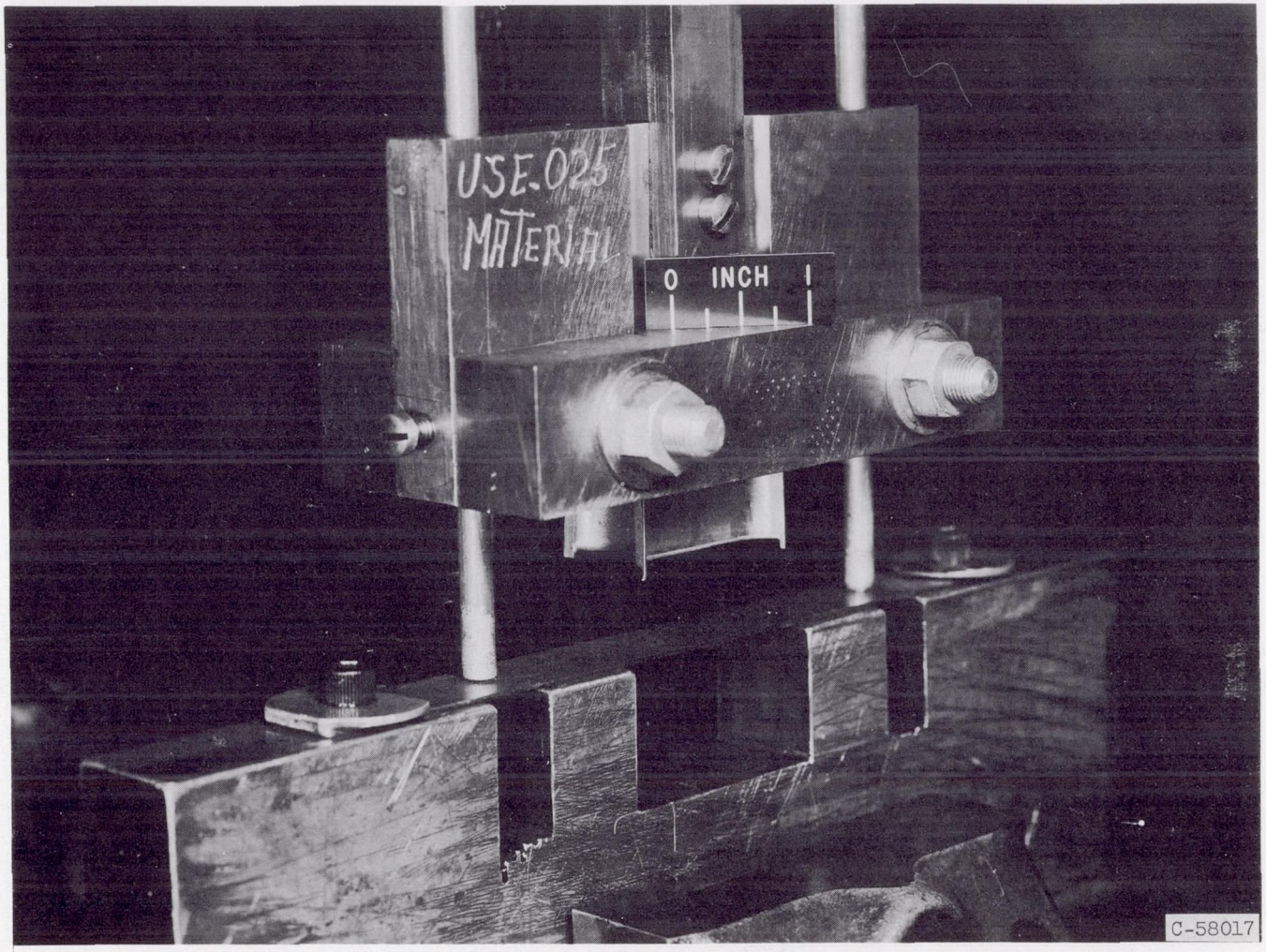

(a) Test bar cutting tool.

Figure 3. - Cutting apparatus for preparation of stress-rupture test specimens.

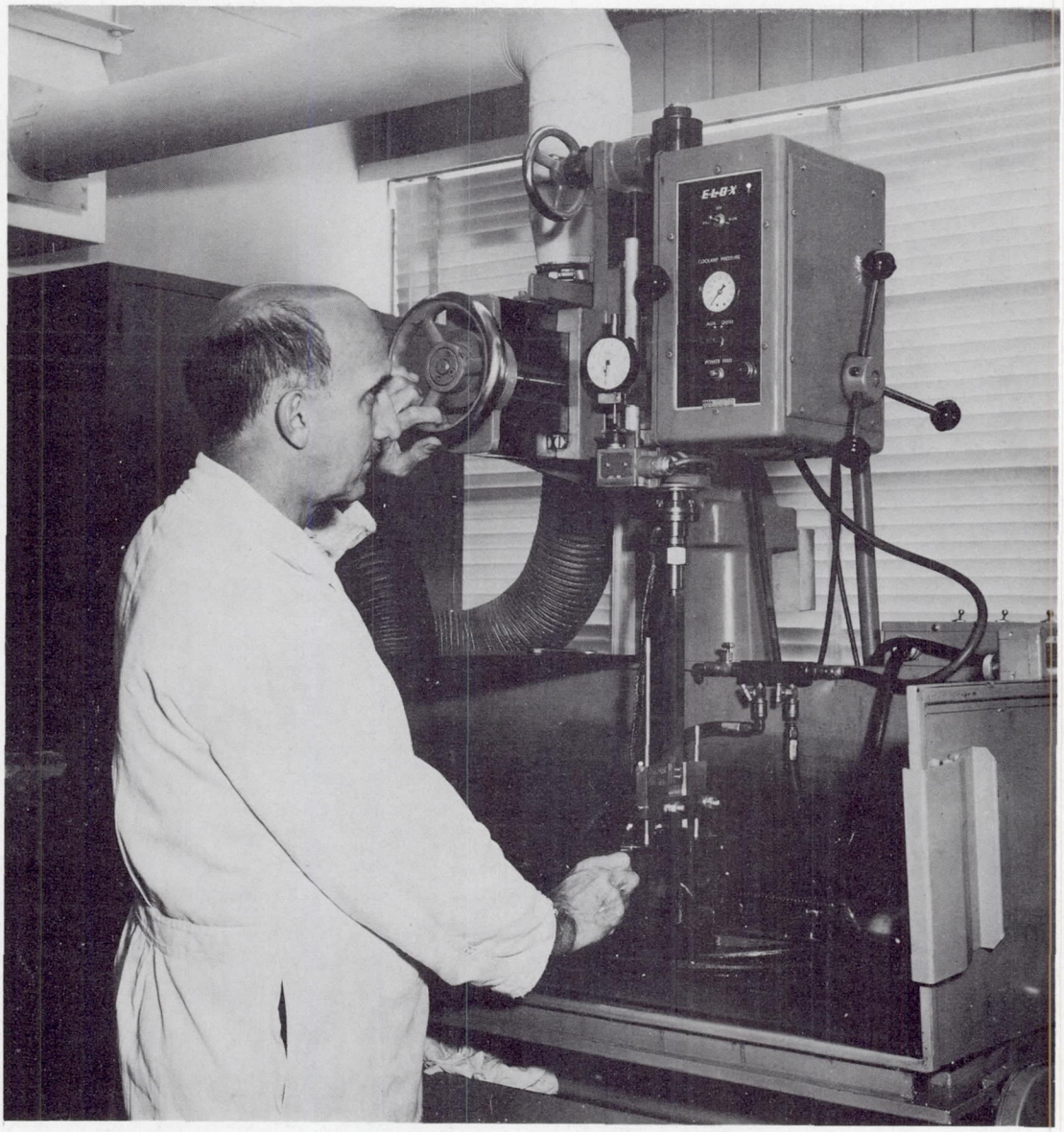

(b) Electric-discharge cutting machine. C-58019

Figure 3. - Concluded. Cutting apparatus for preparation of stress-rupture test specimens.

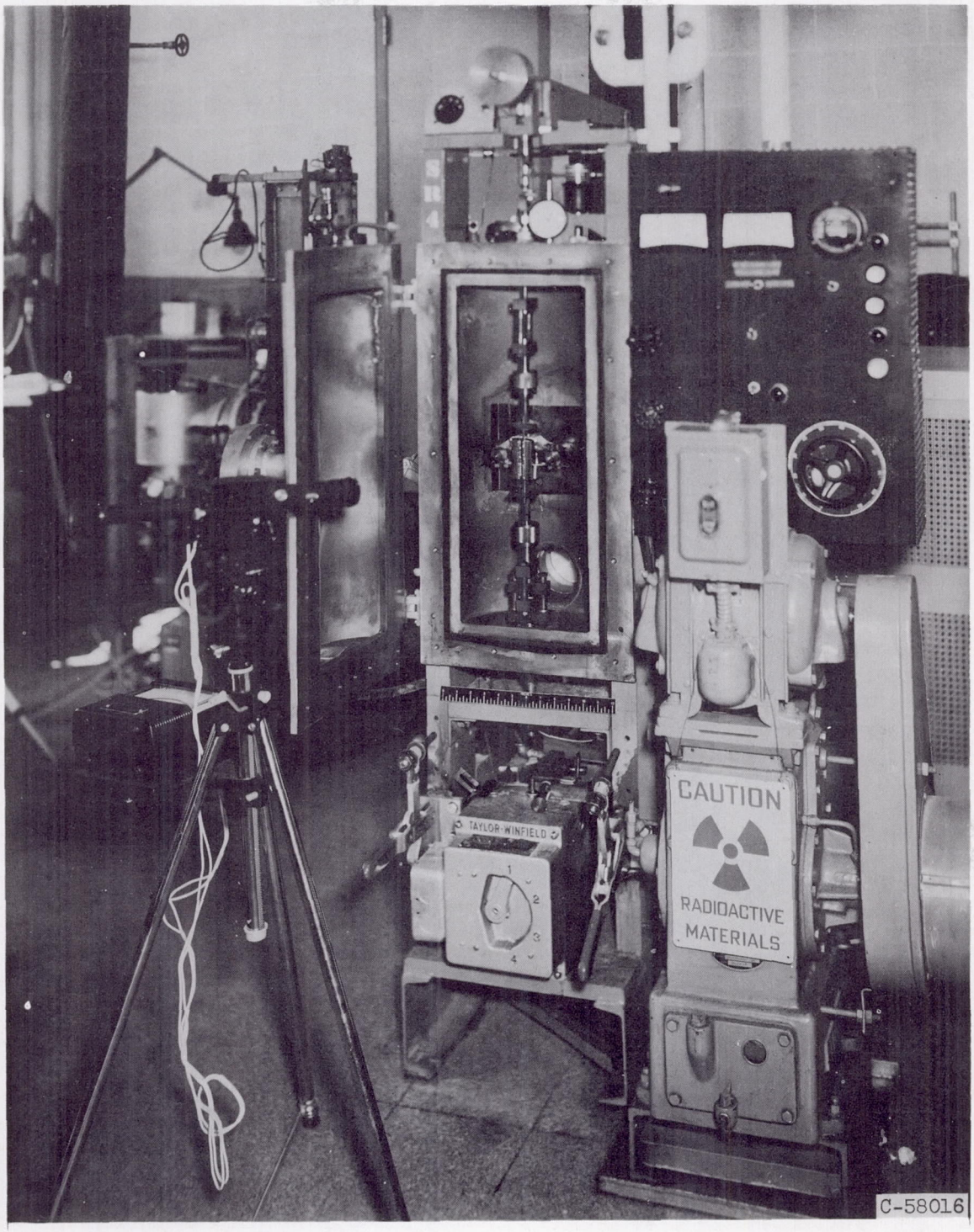

Figure 4. - Stress-rupture apparatus.

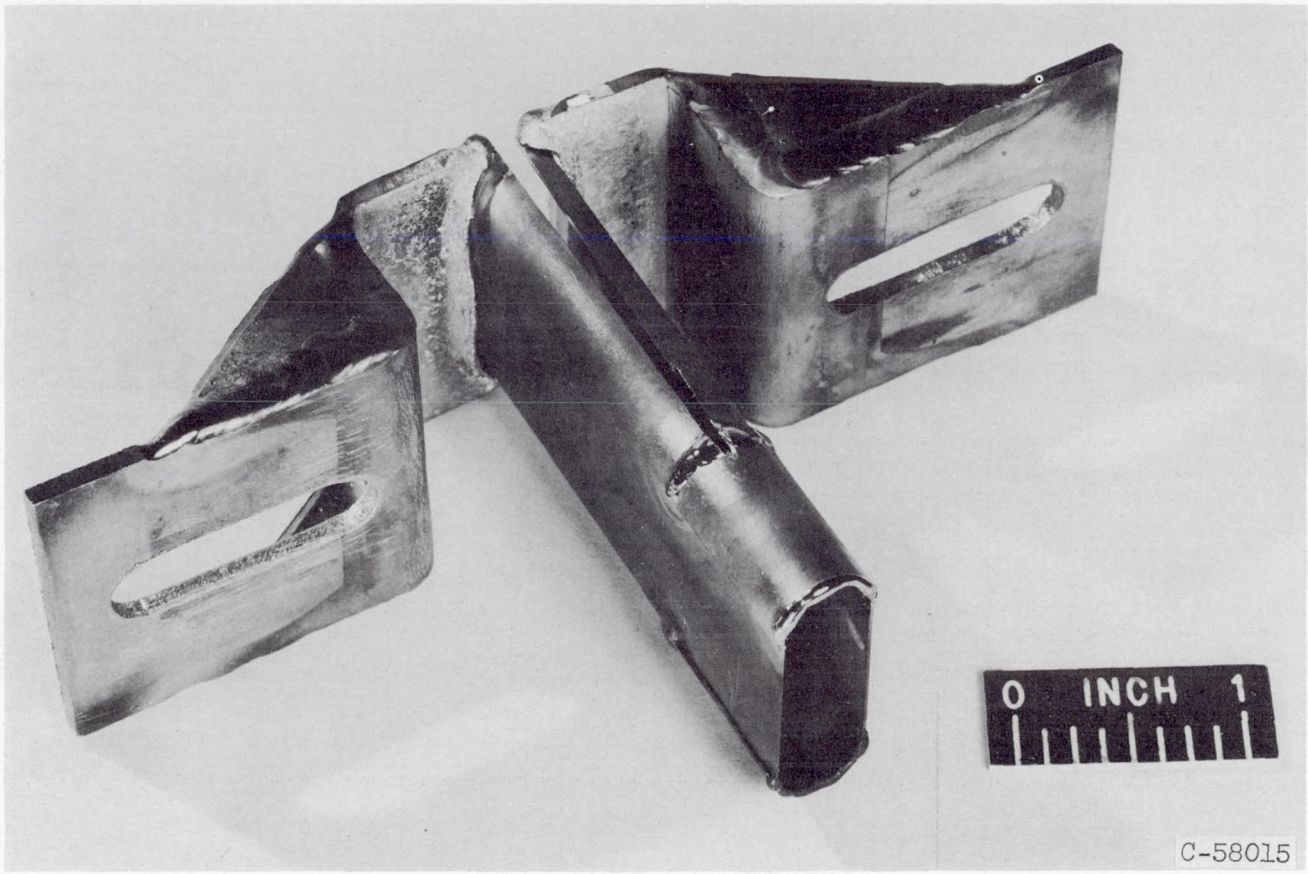

Figure 5. - Tungsten heater used on tensile-testing and stress-rupture machines.

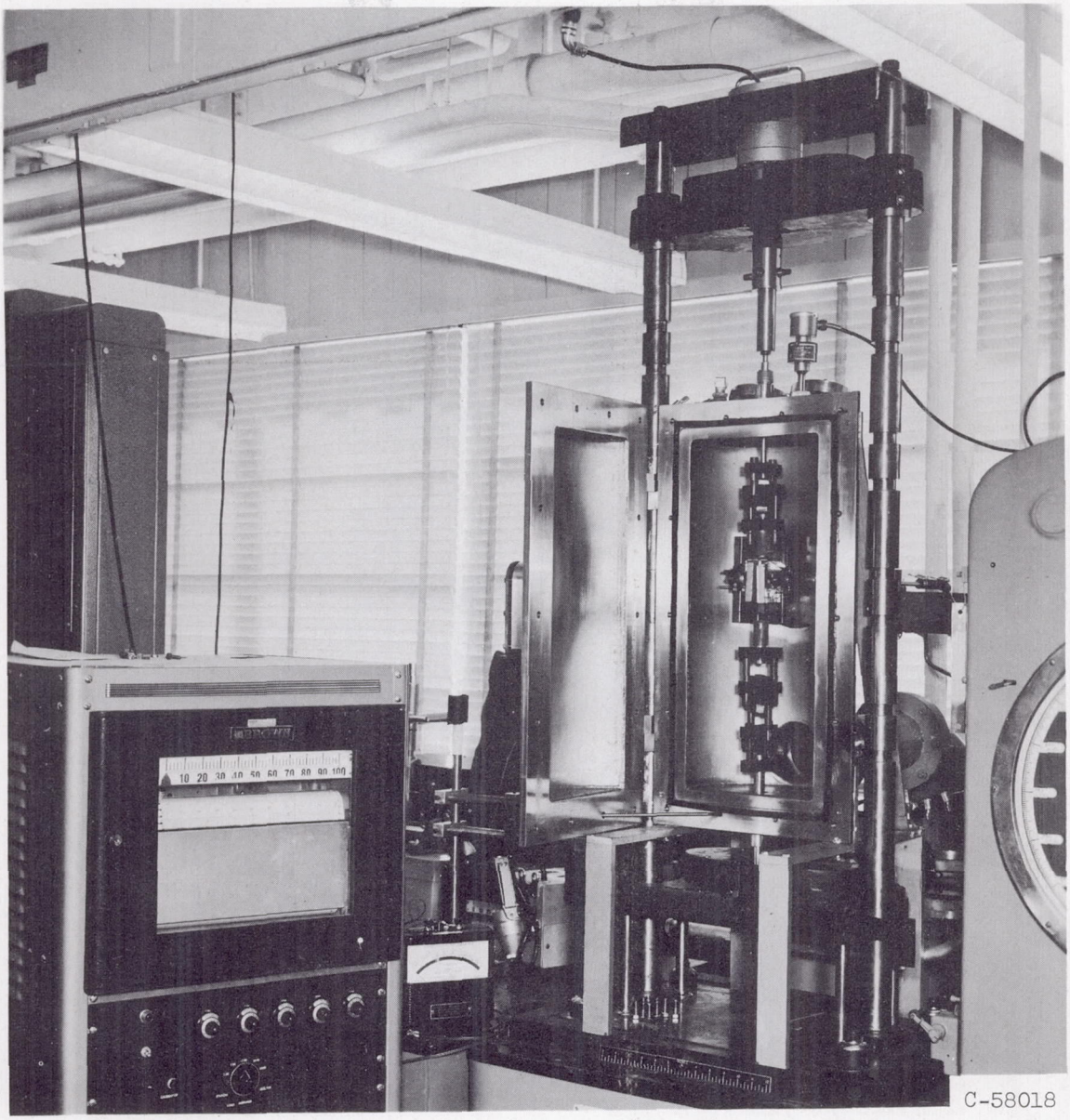

Figure 6. - Tensile test apparatus.

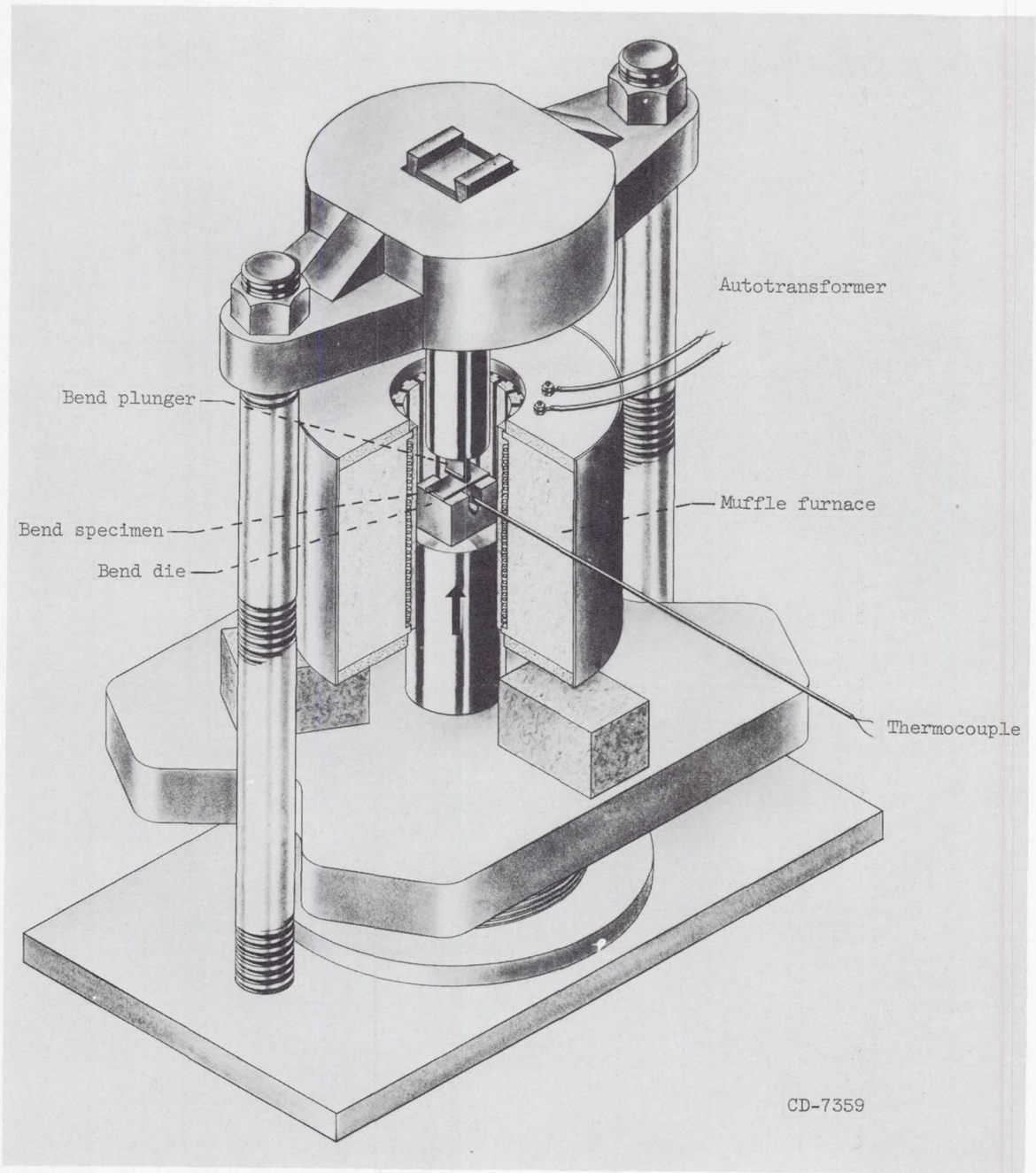

Figure 7. - Bend-test apparatus. Approximately one-quarter scale.

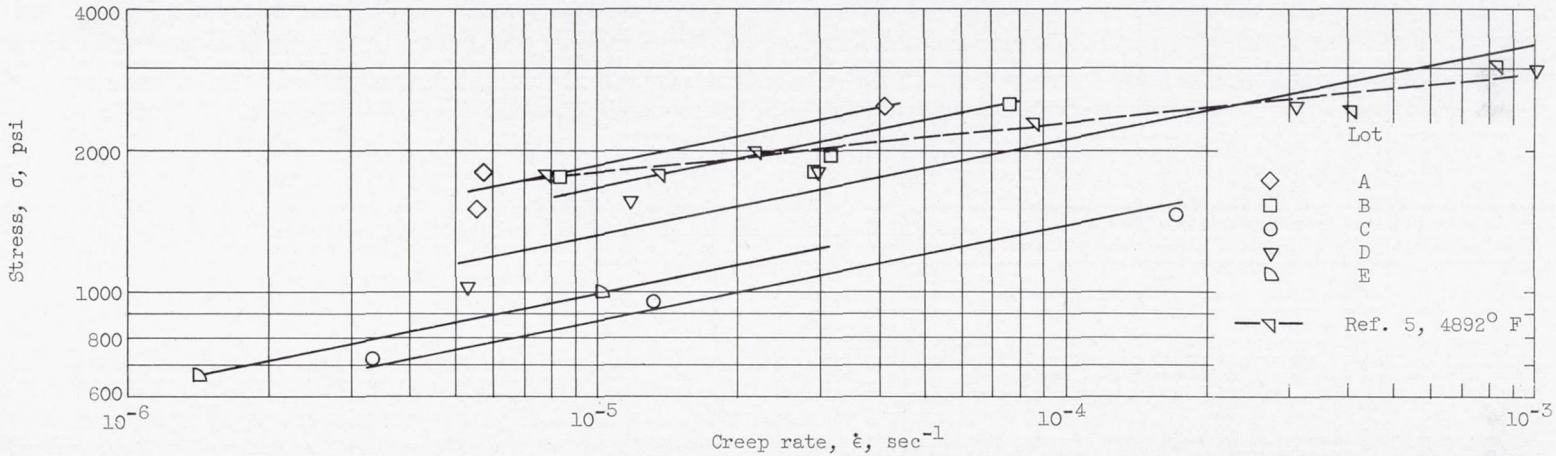

(a) Creep rate.

Figure 8. - Variation of creep rate and rupture life of tungsten with stress at 4800° F.

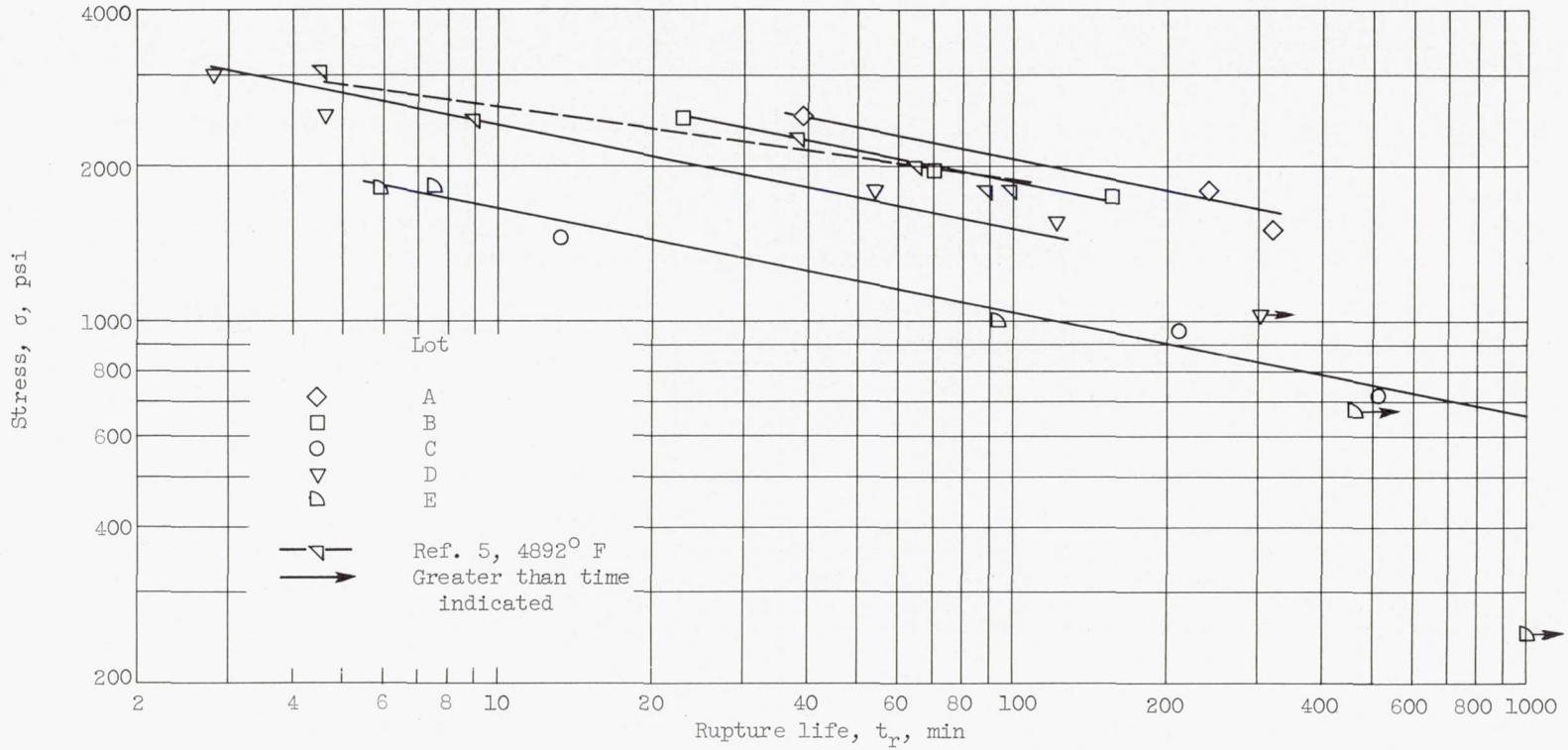

(b) Rupture life.

Figure 8. - Concluded. Variation of creep rate and rupture life of tungsten with stress at 4800° F.

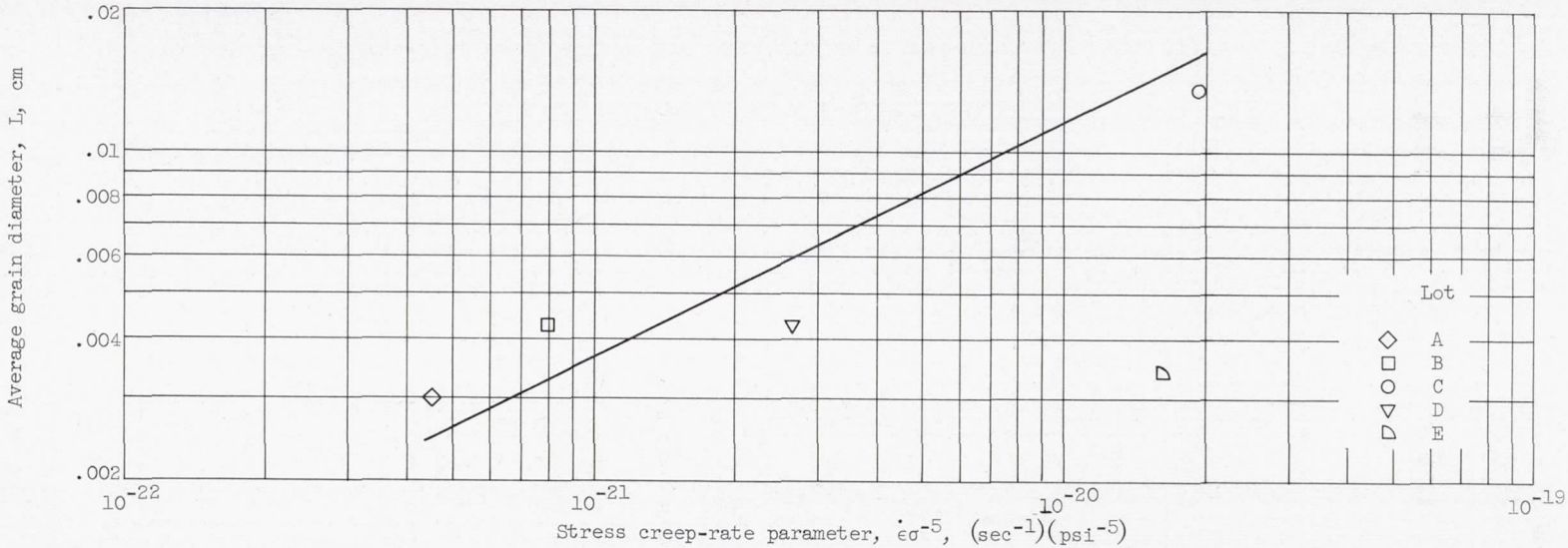

Figure 9. - Variation of average stress creep-rate parameter with average grain diameter for commercial tungsten at 4800° F.

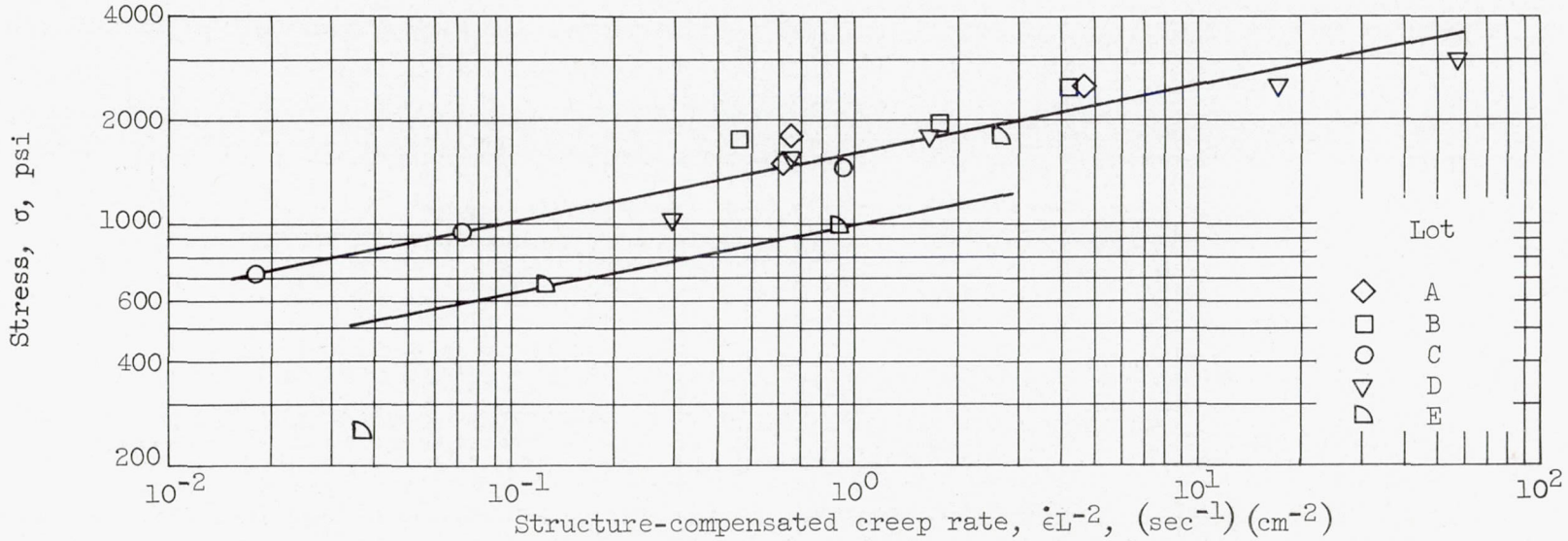

Figure 10. - Variation of structure-compensated creep rate with stress for commercial tungsten at 4800° F.

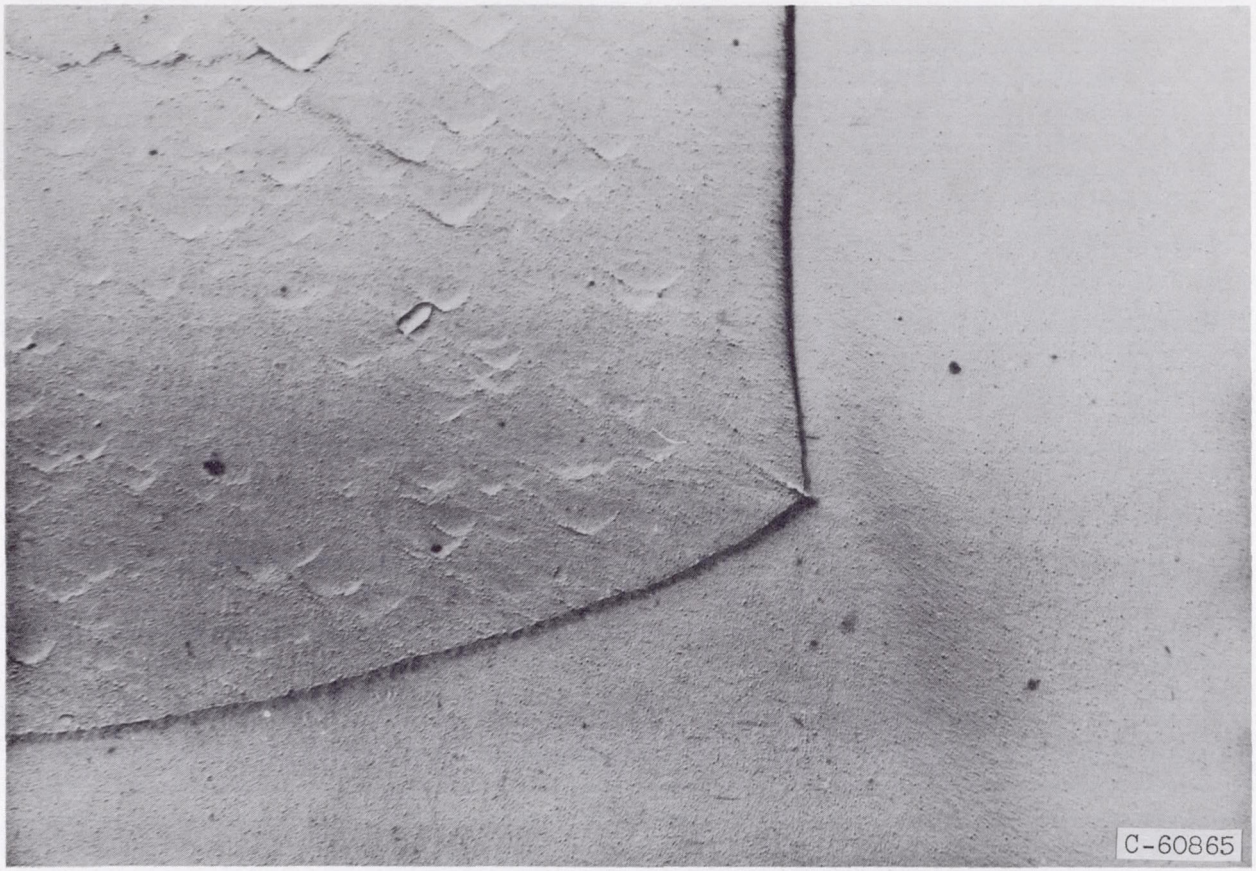

(a) Lot B; X19,000.

Figure 11. - Electron photomicrograph of tungsten after stress-rupture test at 4800° F. Etchant; KOH + $K_3Fe(CN)_6$.

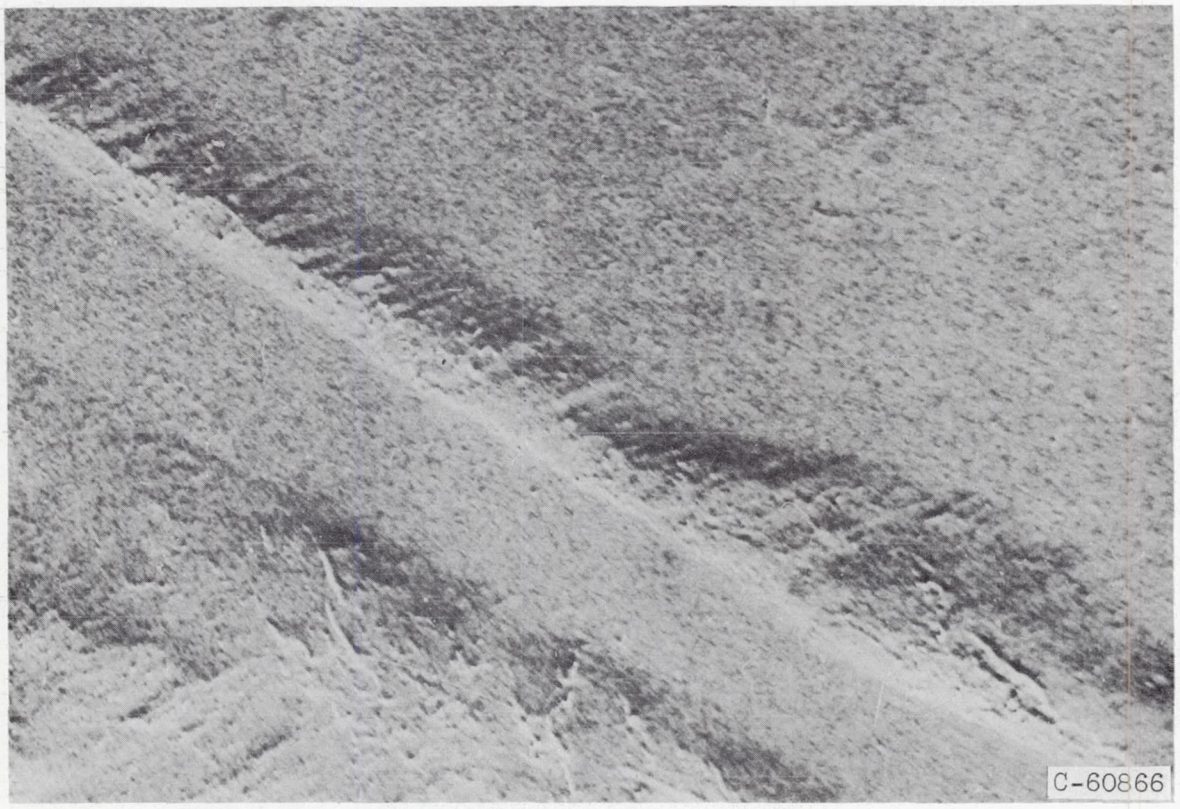

(b) Lot C; X19,000.

Figure 11. - Continued. Electron photomicrograph of tungsten after stress-rupture test at 4800° F. Etchant; KOH + $K_3Fe(CN)_6$.

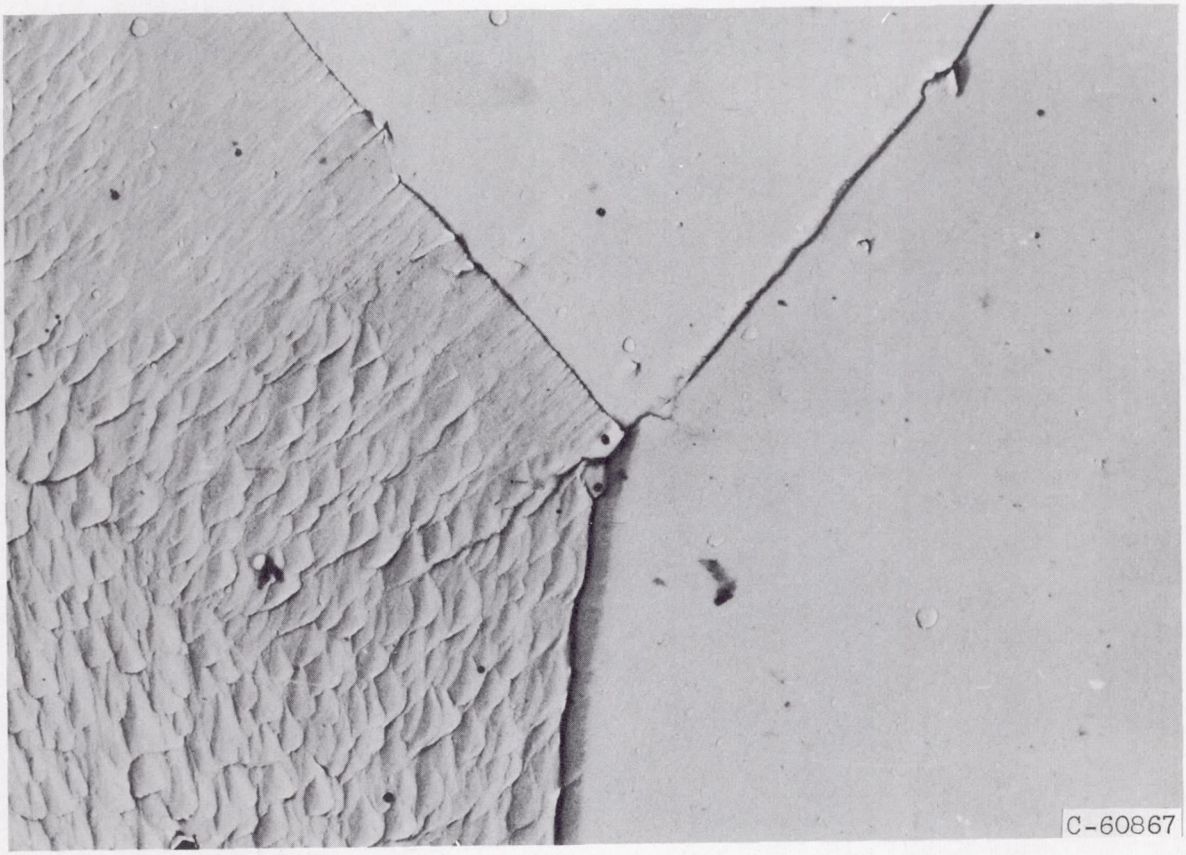

(c) Lot E; X9700.

Figure 11. - Concluded. Electron photomicrograph of tungsten after stress-rupture test at 4800° F. Etchant; KOH + $K_3Fe(CN)_6$.

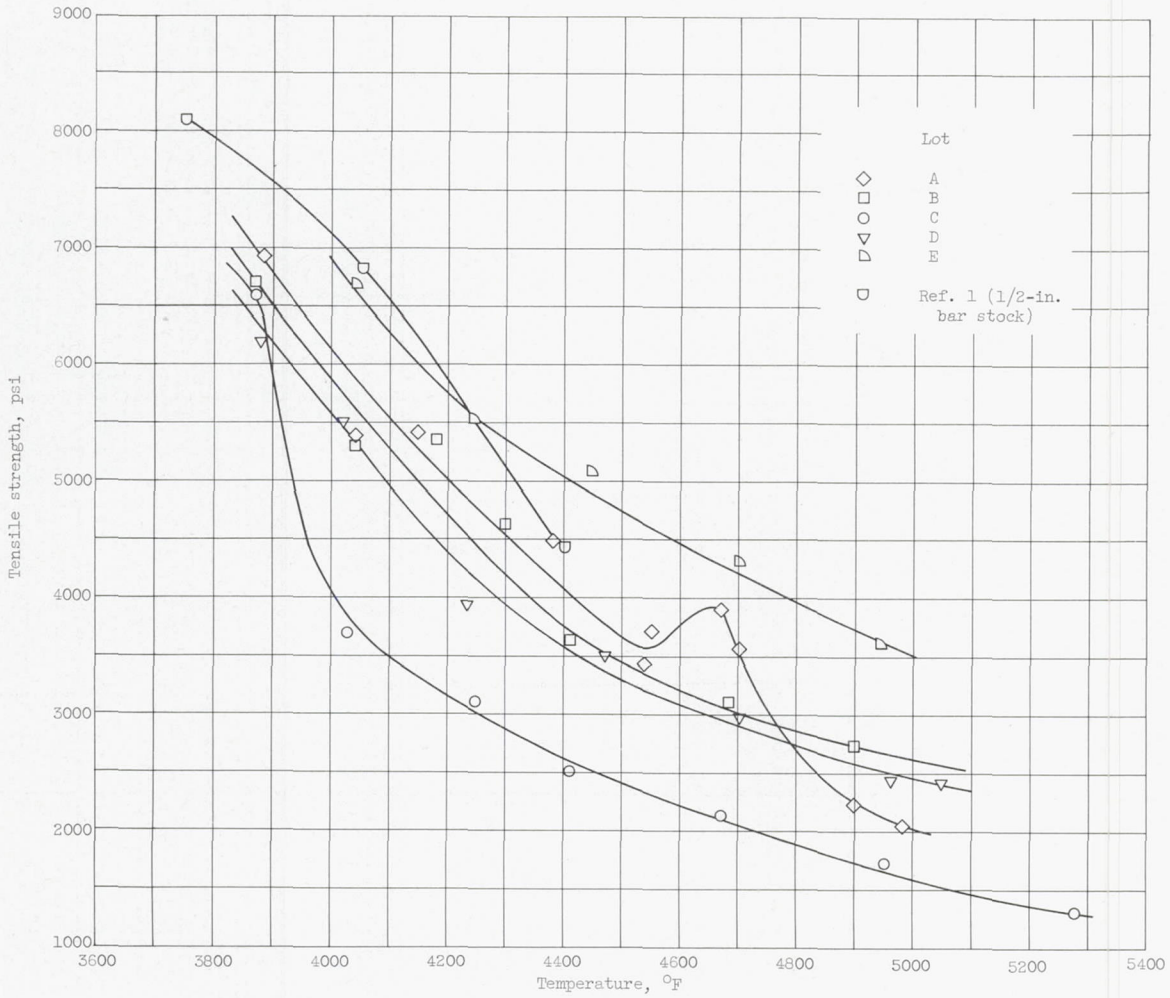

(a) Ultimate tensile strength.

Figure 12. - Variation of strength and ductility of tungsten with temperature.

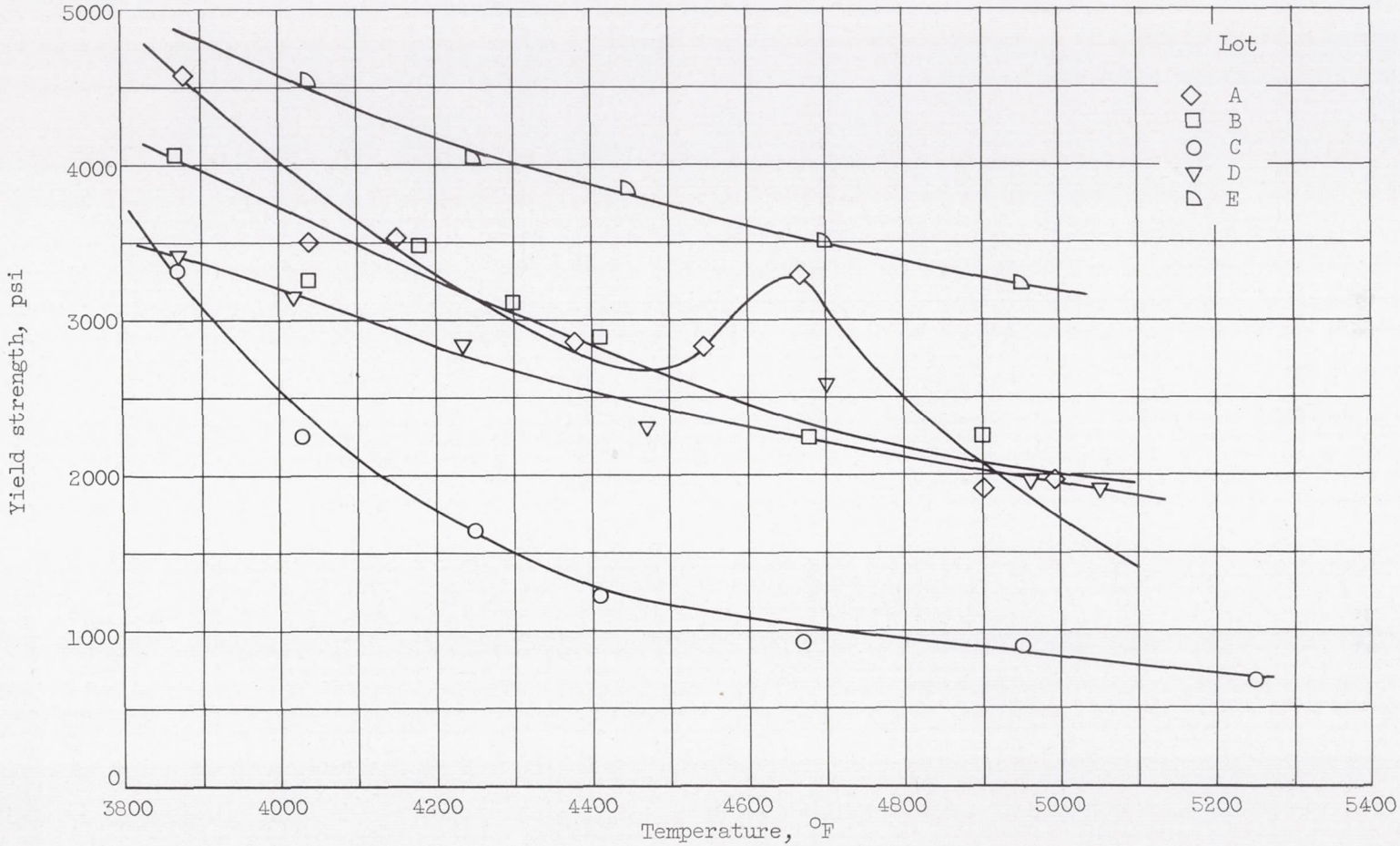

(b) Yield strength.

Figure 12. - Continued. Variation of strength and ductility of tungsten with temperature.

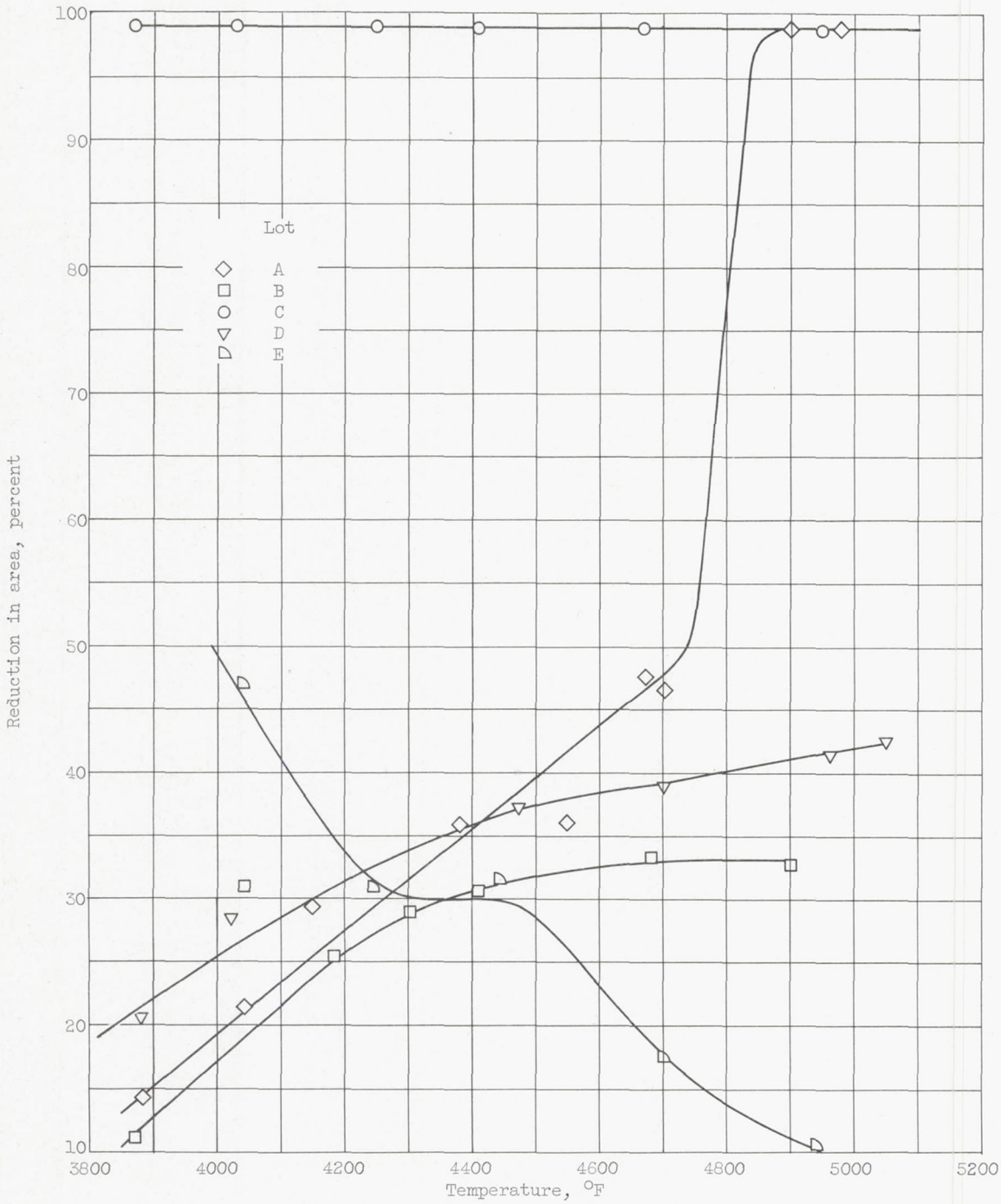

(c) Reduction in area as a measure of ductility.

Figure 12. - Concluded. Variation of strength and ductility of tungsten with temperature.

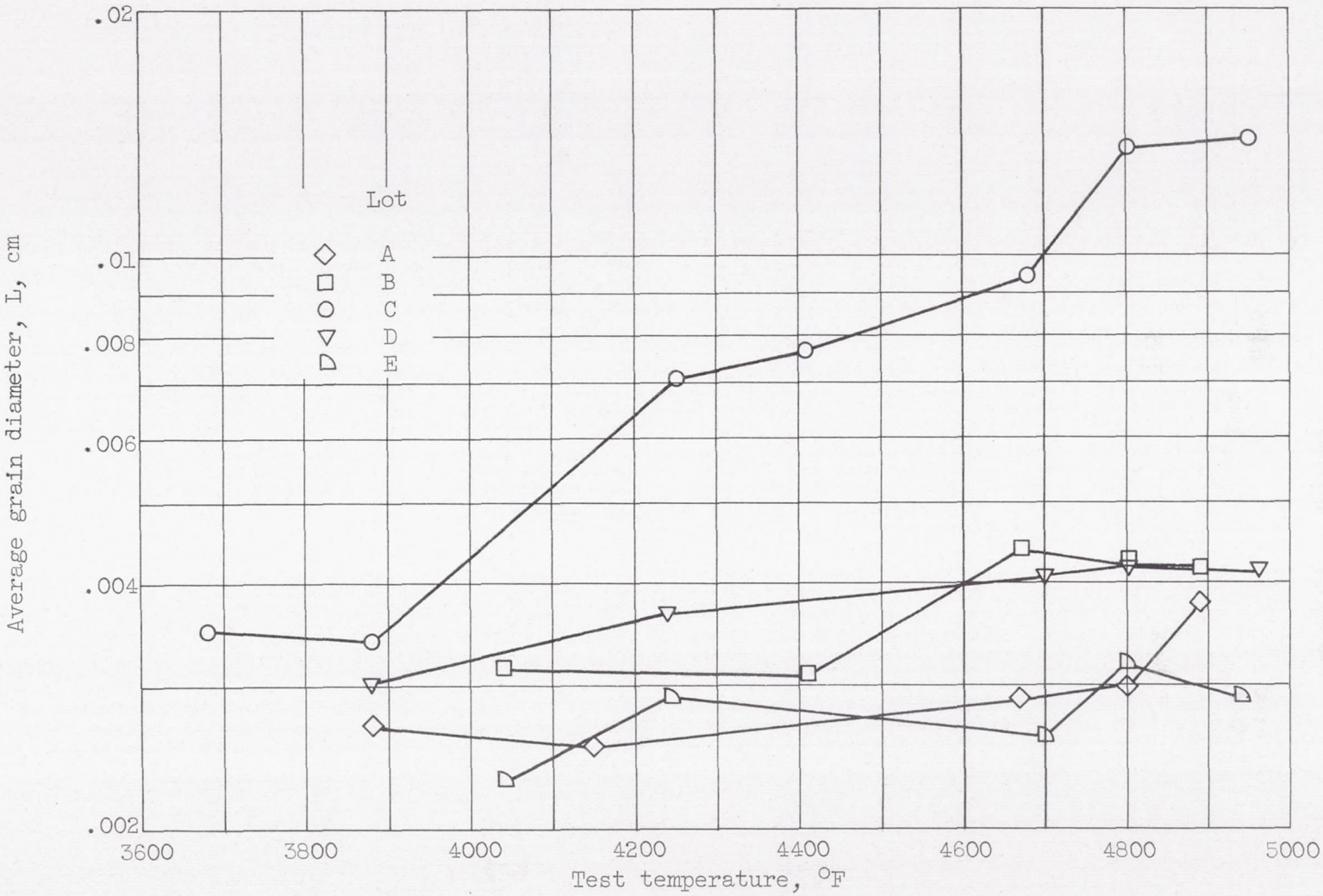

Figure 13. - Average grain diameter of tungsten sheet after high-temperature testing. Data, except those at 4800° F, were obtained from tensile specimens. Data at 4800° F are averages from several stress-rupture specimens.

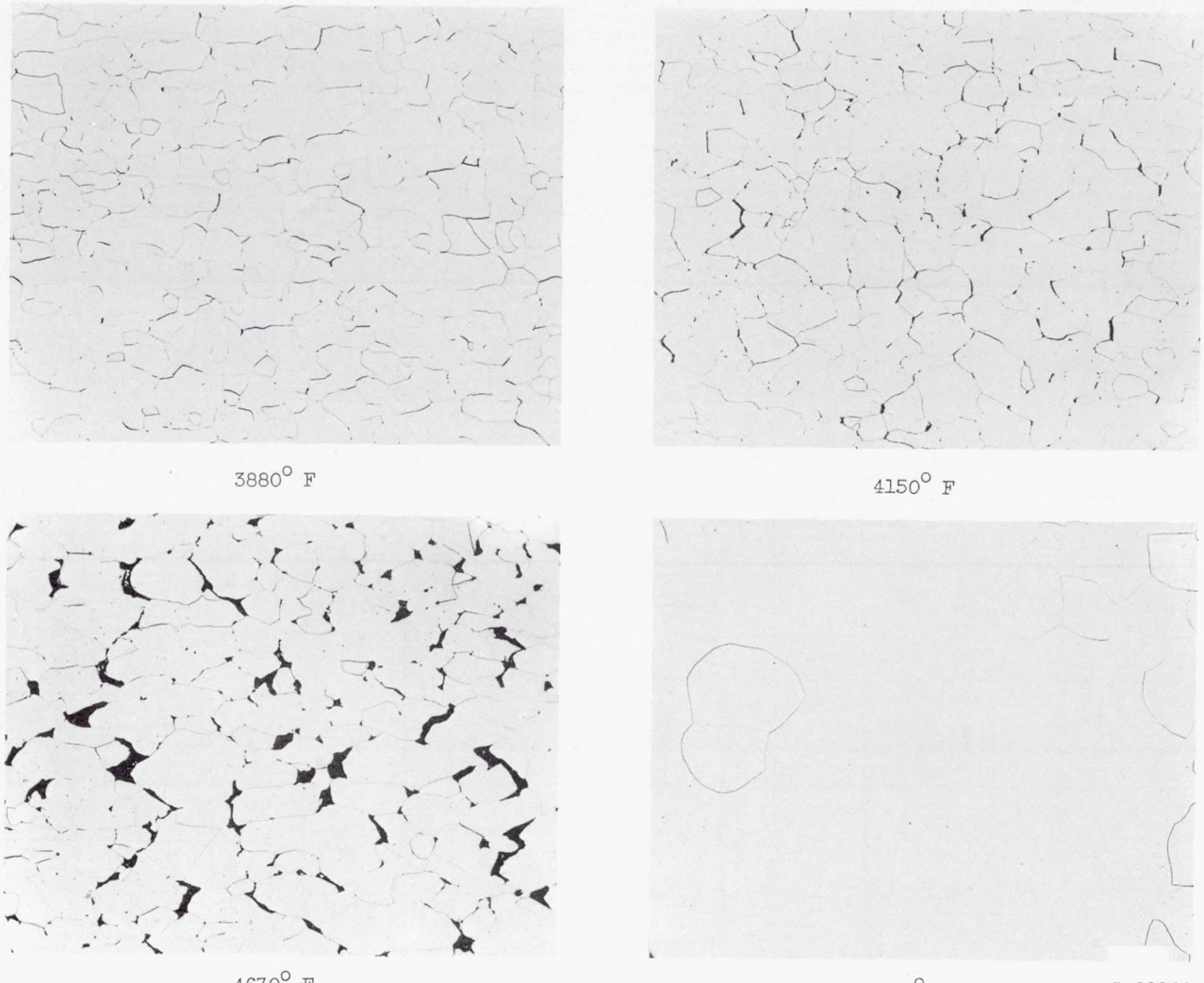

(a) Lot A. Note excessive grain growth at 4900° F.

Figure 14. - Microstructures of tungsten near fracture at high temperatures. Etchant; KOH + $K_3Fe(CN)_6$; X250.

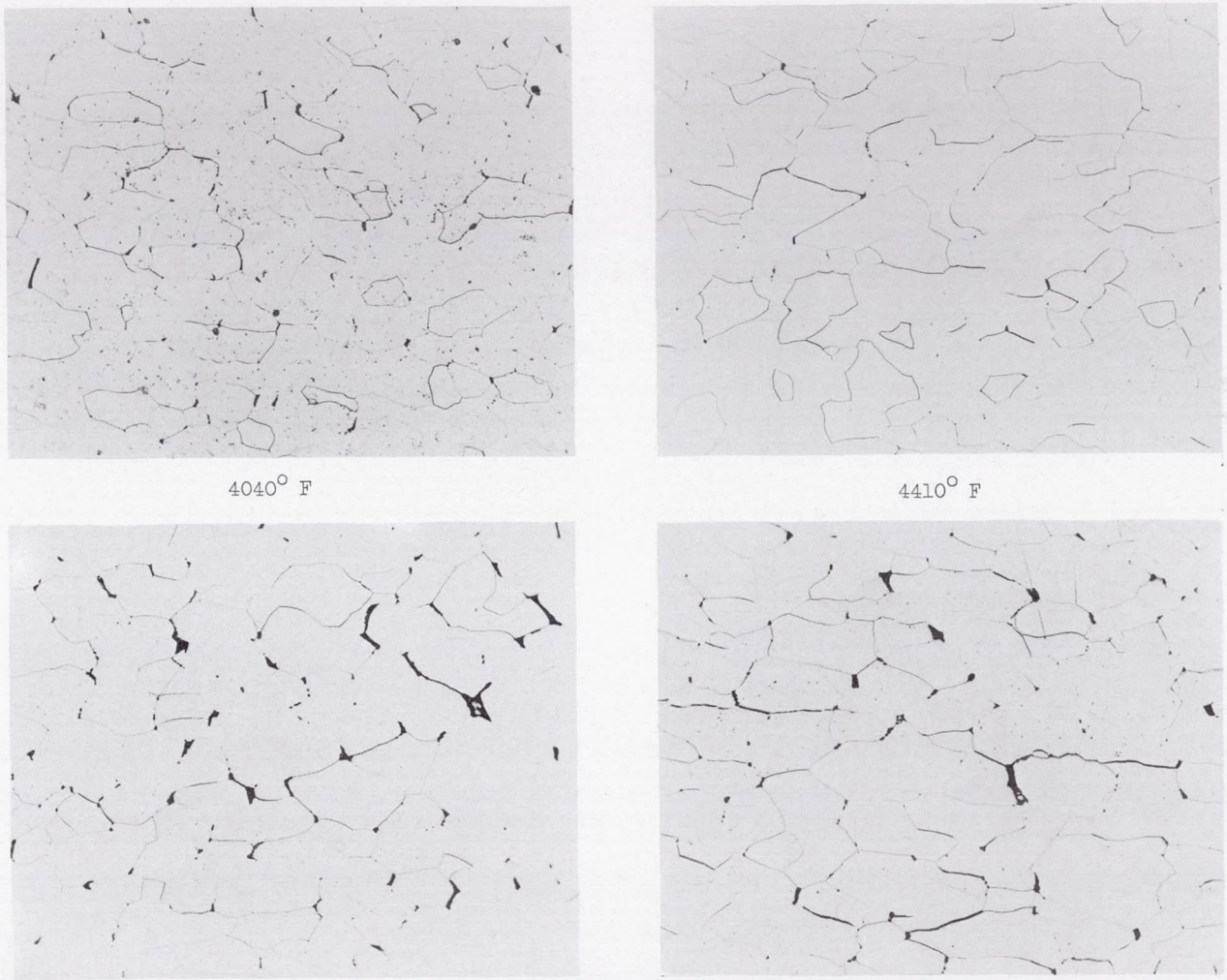

(b) Lot B.

Figure 14. - Continued. Microstructures of tungsten near fracture at high temperatures. Etchant; KOH + $K_3Fe(CN)_6$; X250.

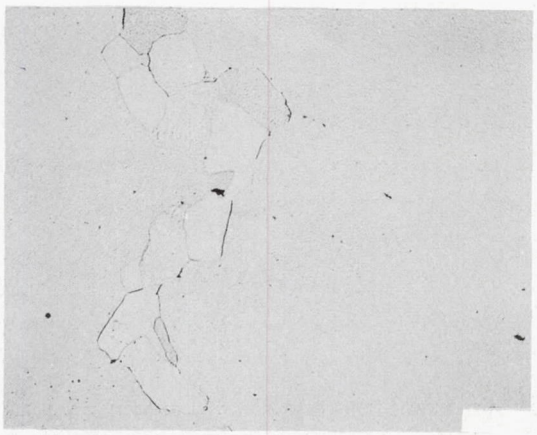

3870° F

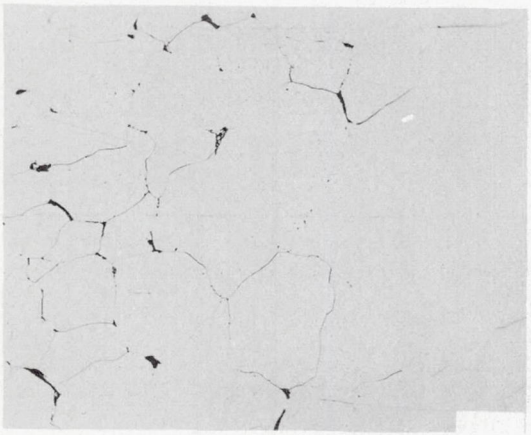

4250° F

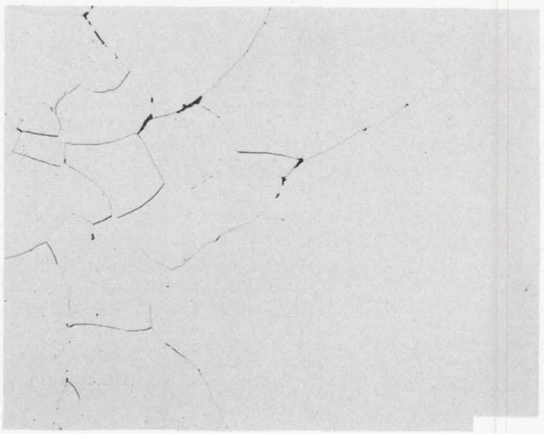

4410° F

4690° F

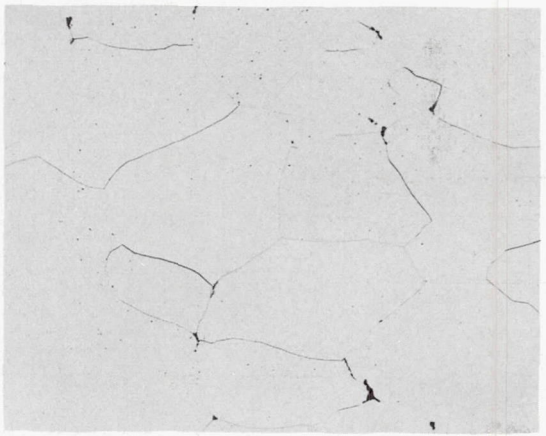

4950° F C-60862

(c) Lot C.

Figure 14. - Continued. Microstructures of tungsten near fracture at high temperatures. Etchant; KOH + $K_3Fe(CN)_6$; X250.

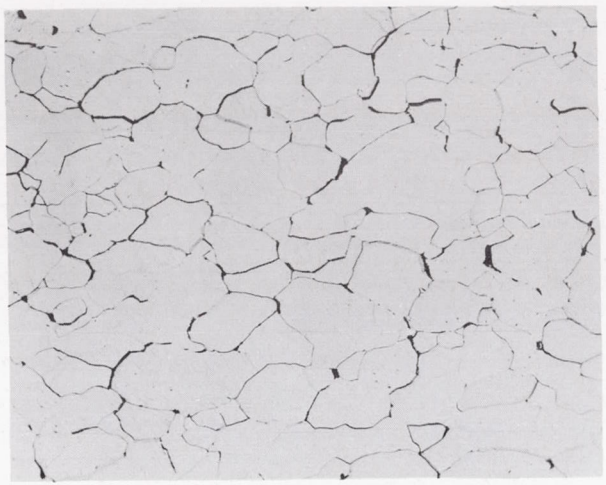

3880° F

4235° F

4700° F

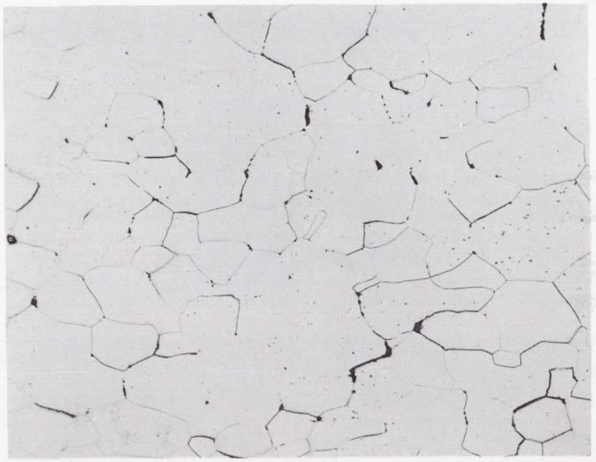

4960° F C-60863

(d) Lot D. Note minor grain growth.

Figure 14. - Continued. Microstructures of tungsten near fracture at high temperatures. Etchant; KOH + $K_3Fe(CN)_6$; X250.

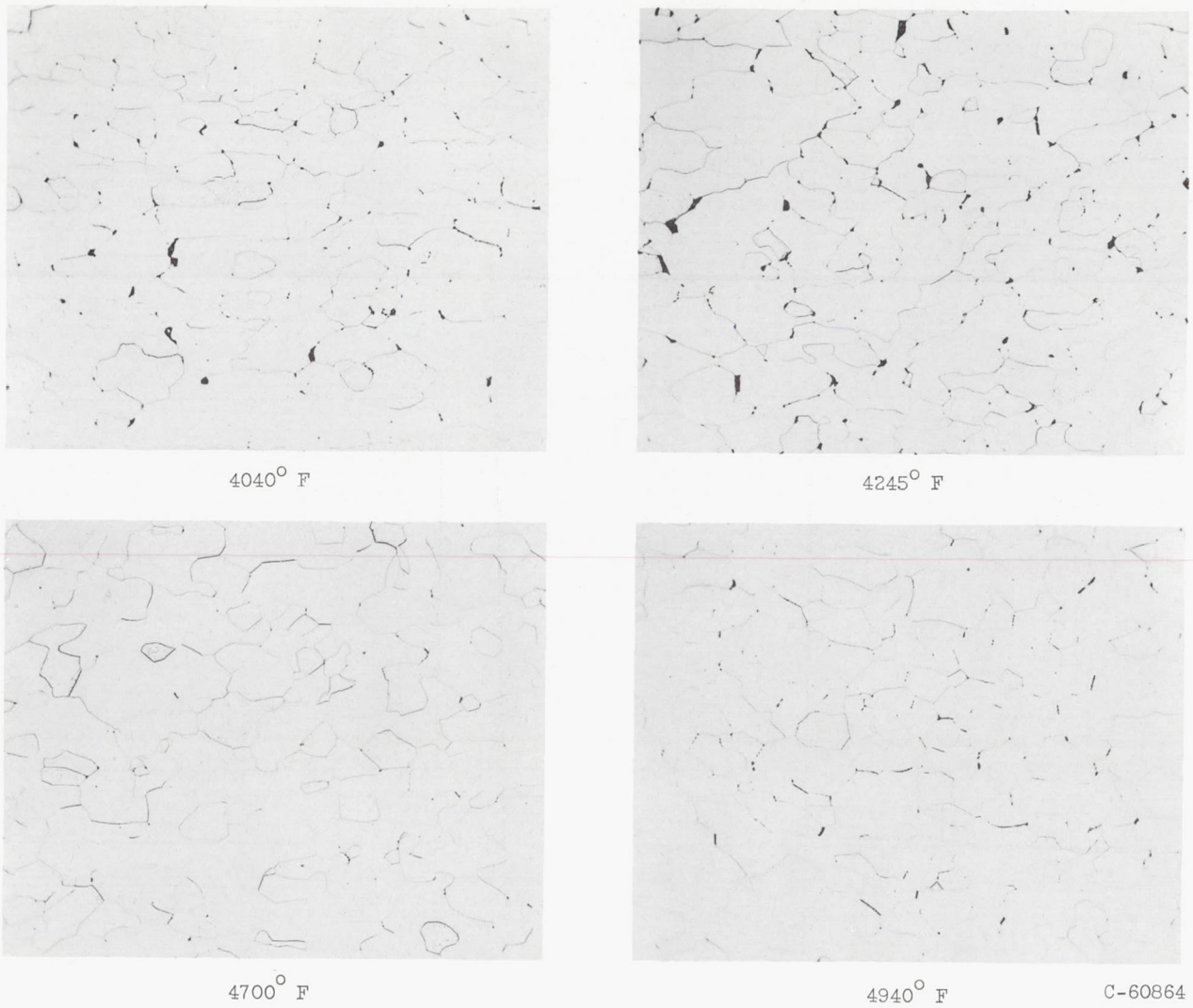

(e) Lot E. Note absence of grain growth.

Figure 14. - Concluded. Microstructures of tungsten near fracture at high temperatures. Etchant; KOH + $K_3Fe(CN)_6$; X250.

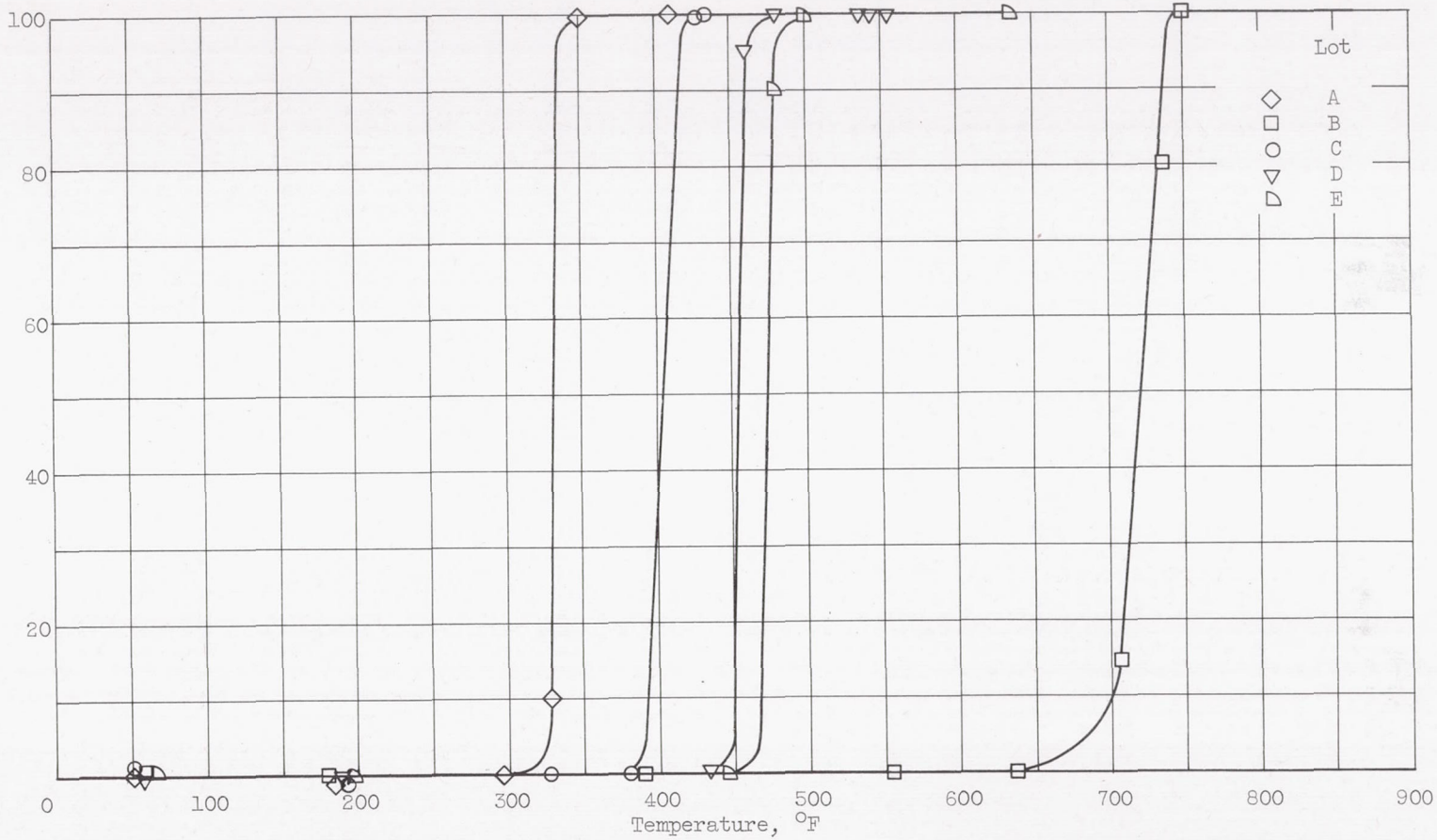

Figure 15. - Transition temperature of bend test for five lots of tungsten sheet. Loading rate, 4 inches per minute; radius, 0.160 inch.

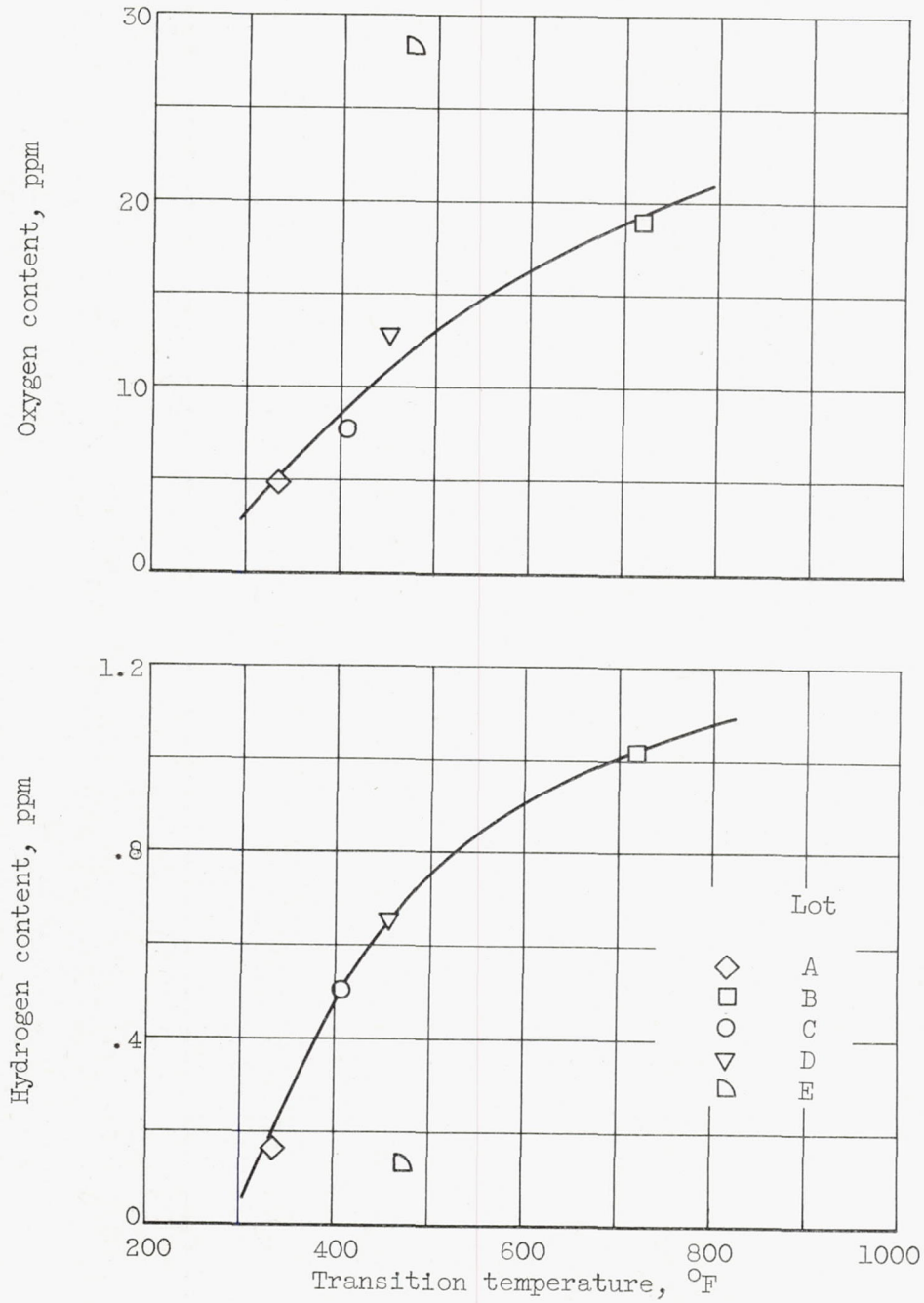

Figure 16. - Transition temperature as function of oxygen and hydrogen content of tungsten.